Ecological Modelling 476 (2023) 110207

Contents lists available at ScienceDirect

Ecological Modelling

journal homepage: www.elsevier.com/locate/ecolmodel

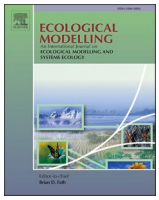

Rabies transmission in the Arctic: An agent-based model reveals the effects of broad-scale movement strategies on contact risk between Arctic foxes

Olivia Tardy [a,d,*], Christophe Lenglos [c], Sandra Lai [b], Dominique Berteaux [b], Patrick A. Leighton [a]

[a] Research Group on Epidemiology of Zoonoses and Public Health, Faculty of Veterinary Medicine, Université de Montréal, 3200 rue Sicotte, Saint-Hyacinthe, J2S 2M2, Quebec, Canada
[b] Canada Research Chair on Northern Biodiversity, Centre for Northern Studies and Quebec Center for Biodiversity Science, Université du Québec à Rimouski, 300 allée des Ursulines, Rimouski, G5L 3A1, Quebec, Canada
[c] McGill University, 3801 rue de l'Université, Montreal, H3A 2B4, Quebec, Canada
[d] Public Health Risk Sciences Division, National Microbiology Laboratory, Public Health Agency of Canada, 3200 rue Sicotte, Saint-Hyacinthe, J2S 2M2, Quebec, Canada

ARTICLE INFO

Keywords:
Arctic rabies
Vulpes lagopus
Spatially explicit agent-based model
Animal movement
Contact rate
Hidden Markov model

ABSTRACT

Arctic rabies is an ongoing threat to human populations and domestic animals inpolar regions, where Arctic foxes (*Vulpes lagopus*) are the main reservoir hosts. Human-driven changes in resource availability are shifting the distribution of Arctic foxes and these changes may affect the risk of rabies transmission and spread. Our understanding of the effects of broad-scale movement strategies in Arctic foxes and spatial distribution of resources on contact patterns among Arctic foxes, and their consequences on the dynamics of rabies epidemiology remains limited, in part, due to the difficulty of obtaining contact data from such remote and expansive regions. In this perspective, we built a spatially explicit agent-based model coupled with hidden Markov models to explore how Arctic fox movement behavior, combined with Arctic fox population density, resource availability and rabies transmission dynamics, affects the risk of infectious contact between Arctic foxes across heterogeneous landscapes. The model was parameterized using a combination of unique field data collected in the Canadian High Arctic and published studies from other Arctic regions. A sensitivity analysis was performed to assess the effects of multiple model input parameters on contact rates among Arctic foxes. Our results showed that cumulative contact rates per fox were driven by predictors related to rabies transmission dynamics and fox carrying capacity, while unique contact rates per fox and unique infectious contact rates per rabid fox were best predicted by parameters associated with rabies transmission dynamics, fox movement behavior, and fox carrying capacity. Ultimately, our study provides new insights into the ecological drivers of rabies transmission and may inspire further research on modelling cost-effective rabies prevention strategies in the Arctic.

1. Introduction

Heterogeneity in the rate at which infectious individuals come into contact and transmit pathogens to susceptible individuals plays a key role in infectious disease dynamics (Wilson et al., 2002). Some hosts can contribute disproportionately to pathogen spread, which can lead to "super-spreading" events (Lloyd-Smith et al., 2005). Woolhouse et al. (1997) proposed the 20/80 rule, whereby 20% of the most infectious hosts in a given population are responsible for at least 80% of pathogen transmission. Because heterogeneity in pathogen transmission has major implications for disease management and prevention (VanderWaal and Ezenwa, 2016), it is important to identify the mechanisms inducing individual variation in the probability of transmitting pathogens given contact. Differences in physiology and behavior among hosts can contribute to such variation in pathogen acquisition (VanderWaal and Ezenwa, 2016).

Host behavior is an important component for directly transmitted diseases (i.e., those requiring contact between a susceptible and an infectious individual), in particular when space use patterns affect the contact risk among potential hosts (Johnson and Hoverman, 2014; VanderWaal and Ezenwa, 2016). While social interactions can induce large variation in contact rates between individuals and create situations that facilitate pathogen transmission in the landscape (Altizer et al., 2003), movement patterns can also influence the number of contacts

* Corresponding author.
E-mail address: olivia.tardy@umontreal.ca (O. Tardy).

https://doi.org/10.1016/j.ecolmodel.2022.110207
Received 30 September 2022; Accepted 3 November 2022
Available online 30 November 2022

between individuals. Movement behavior can be characterized at different temporal and spatial scales (Benhamou, 2014). At coarse temporal resolutions, animal movement is often categorized into four strategies (migration, dispersal, nomadism, and sedentarism; *sensu* Bastille-Rousseau et al., 2016), while at finer temporal scales, movement can be classified as behavioral states (e.g., resting, searching, foraging) (Fryxell et al., 2008). Changes in movement behavior are driven by trade-offs between the costs of moving (e.g., energy loss, risk of mortality) and the benefits of resource acquisition (Bonte et al., 2012), and these changes can affect infectious disease dynamics in wildlife. While the interest of understanding the causes and ecosystem-level consequences of broad-scale animal movement strategies has led to the development of multiple modeling approaches (reviewed in Joo et al., 2020), few studies have explored the effects of different broad-scale host movement strategies on zoonotic pathogen transmission (e.g., migration vs. sedentarism; Pruvot et al., 2016; Rayl et al., 2021). There are thus opportunities to use movement-based behavioral analyses to explore pathogen transmission risk among individuals (Dougherty et al., 2018).

Rabies is one of the most widespread zoonotic diseases that threaten human and animal health (Fooks et al., 2014). This virus is responsible for approximately 59,000 human deaths worldwide and 8.6 billion US dollars in economic losses per year (Hampson et al., 2015). Several distinct strains of rabies virus circulate in multiple species of wild mammals (Baer, 1991; Warrell and Warrell, 2004). The Arctic strain of rabies is observed throughout Arctic and sub-Arctic regions, where the virus remains enzootic in wildlife (Crandell, 1991), thus posing a significant threat to public health (Mediouni et al., 2020). A person can contract rabies following a bite by a rabid wild animal or a domestic dog that became infected as a result of contact with a rabid wild animal (Mørk and Prestrud, 2004). The Arctic fox (*Vulpes lagopus*) is regarded as the primary reservoir host for Arctic rabies (Mørk and Prestrud, 2004; Simon et al., 2020). Arctic foxes are both opportunistic predators and scavengers of a wide variety of prey, and have a circumpolar distribution that spans inland and coastal habitats varying in rodent availability, which induces differences in feeding strategies (Angerbjörn et al., 2004). Arctic foxes relying on rodents, such as lemmings, are highly dependent on cyclical rodent population pulses occurring every three to five years (Bêty et al., 2002). Consequently, these lemming foxes can have large litters (up to 19 cubs) but show high variation in breeding success (Tannerfeldt and Angerbjörn, 1998). In contrast, Arctic foxes living in coastal habitats where cyclic rodents are absent, like Svalbard, Iceland and West Greenland, have access to relatively stable and predictable food resources among years, and their diet is diversified consisting of many marine food items that are largely available in summer, but limited in winter (e.g., carcasses of marine mammals and seabirds, crustaceans, and fishes) (Berteaux et al., 2017; Hersteinsson and Macdonald, 1996; Prestrud, 1992). Consequently, these foxes produce fewer cubs per litter and their reproduction patterns are more stable compared to lemming foxes (Tannerfeldt and Angerbjörn, 1998). Resource availability also has a large influence on movement behavior of Arctic foxes. It has been suggested that lemming foxes may travel longer distances than coastal ones in response to food shortages (Angerbjörn et al., 2004). In this context, changes in Arctic fox movement behavior could affect the risk of contact between individuals, with implications for rabies virus transmission. Several rabies models, often involving raccoons, red foxes, skunks and bats, have been used to investigate the influence of host density, host behavior (including movement and habitat selection) and landscape features (i.e., landscape composition and configuration) on rabies transmission and spread dynamics or contact risk (Brunker et al., 2018; Sararat et al., 2022; Smith et al., 2002; Tardy et al., 2018), and to test rabies control strategies (McClure et al., 2022, 2020; Newton et al., 2019). However, we lack an understanding of how Arctic fox movement behavior affects Arctic rabies transmission dynamics, partly due to the difficulty of obtaining contact data from remote and expansive areas of Arctic and sub-Arctic regions. In addition, the majority of existing Arctic rabies models do not explicitly incorporate mechanistic links between Arctic fox movement and landscape heterogeneity (Moran et al., 2021, 2022; Simon et al., 2019), which can lead to less accurate predictions of transmission events (Fofana and Hurford, 2017).

We built a spatially explicit agent-based model (ABM) coupled with hidden Markov models to explore how broad-scale Arctic fox movement strategies, in concert with Arctic fox population density, spatial distribution of resources and rabies transmission dynamics, affect the risk of virus transmission among Arctic foxes across spatially heterogeneous landscapes. The objective of this study was addressed in two steps. First, we identified different broad-scale Arctic fox movement strategies using multi-year Argos satellite data. Then, we quantified the relative influence of multiple ABM input parameters and explored their relationships with different metrics of contact rates, through a global sensitivity analysis. Using the ABM, we simulated Arctic fox populations varying in broad-scale movement strategies and individual densities across theoretical landscapes that differed in spatial aggregation of resources.

2. Materials and methods

2.1. Characterization of broad-scale movement strategies

We identified broad-scale movement strategies in 41 satellite-tracked Arctic foxes using net squared displacement (NSD) statistics with a discrete latent state model (a type of hidden Markov model) (Bastille-Rousseau et al., 2016) (see the subsection "Model parameterization" for more details on telemetry data). The approach combining NSD statistics and a latent state model consisted in calculating NSD values from Argos-derived locations for each individual and fitting the frequency distribution of the NSD values with a latent state model based on a mixture of two normal distributions and one pseudo-uniform distribution (Bastille-Rousseau et al., 2016). The NSD is calculated as the square of the Euclidean distance between the first location of an individual and each subsequent location of its movement path (Bunnefeld et al., 2011; Turchin, 1998). A latent state model defines three movement modes based on the frequency distribution of the NSD values: two encamped modes (1 and 2) that correspond to different foraging areas where movements are slow and meandering, and one exploratory mode (3) that is equivalent to a transitional movement mode allowing for fast and directed movements between these areas (Bastille-Rousseau et al., 2016). The modes 1 and 2 are characterized by a normal distribution of the NSD values, while the mode 3 is defined by a pseudo-uniform distribution of the NSD values (Bastille-Rousseau et al., 2016). The latent state model takes into consideration the temporal autocorrelation present in NSD time-series, and satisfies the Markov property according to which the behavioral state at a given time depends on the state at the previous time, which makes it possible to investigate the probabilities of switching between movement modes (see Bastille-Rousseau et al., 2016 for the full expression of the likelihood of the latent state model). The criteria used to differentiate movement strategies are based on a 3×3 matrix representing the probability of being in movement mode j at time $t + 1$ given that the individual was in mode i at time t (q_{ij}) for $i.j \in \{1,2,3\}$, and the number of transitions between each mode (see Bastille-Rousseau et al., 2016 for further details). A Bayesian modeling framework based on Markov chain Monte Carlomethods is used for estimating parameters (Bastille-Rousseau et al., 2016). For each fox, we ran a model using three Markov chains and 5000 iterations. When the model did not converge, we reran the model by increasing the number of iterations (up to 250,000 iterations). The model was validated by visually comparing the NSD time-series to those in Bunnefeld et al. (2011) (double-sigmoid function = migration, sigmoid function = dispersal, linear function = nomadism, and horizontal asymptotic function = sedentarism; see also Fig. 1 in Bastille-Rousseau et al., 2016). Finally, we tested how the characterization of movement strategies was sensitive to the starting date of the NSD time-series using a clustering technique (see Bastille-Rousseau et al., 2016 for more details). We varied the start date over the first 70 days of locations by taking 10 windows of locations of 7

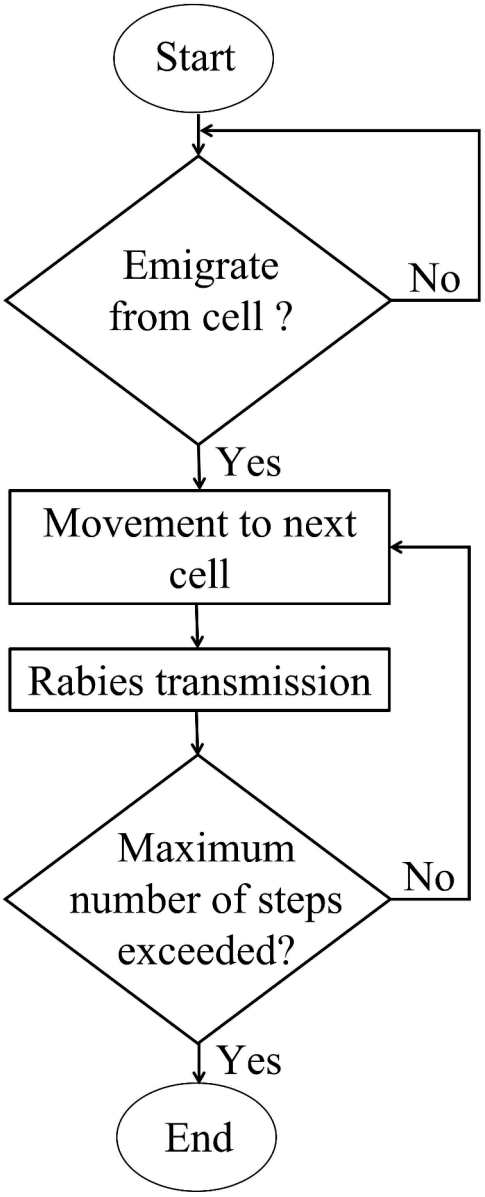

Fig. 1. Process overview. Flowchart of the ABM illustrating actions (rectangles) and decisions (diamonds).

days, and we ran the models with 25,000 iterations. The analysis of movement strategies using NSD statistics with a latent state model was performed with the *lsmnsd* package (version 0.0.0.9000; Bastille-Rousseau et al., 2016) in the R statistical software (version 3.6.1; R Development Core Team, 2019).

2.2. Model overview

In this section, we provide a detailed ABM description following the Overview, Design concepts and Details (ODD) protocol (Grimm et al., 2006, 2010, 2020). The model was implemented in R using the *NetLogoR* package (version 0.3.7; Bauduin et al., 2019).

2.2.1. Purpose and patterns

The ABM is designed to simulate broad-scale movement strategies of Arctic foxes from hidden Markov models (HMMs) that were parameterized with telemetry location data and in which we incorporated covariates. Using this modeling framework in an epidemiological context, the purpose of the ABM is to identify the primary drivers of the risk of rabies transmission between Arctic foxes among host-specific (movement and carrying capacity), environmental (resource availability) and epidemiological predictors, and to explore their relationships across spatially heterogeneous landscapes. Given that rabies transmission events are broadly dependent on mechanisms modulating contact rates, we explored cumulative and unique contact patterns among simulated Arctic foxes emerging from the mechanistic movement process implemented in the ABM. The integration of a rabies transmission process in the ABM provides the possibility of evaluating the risk of rabies transmission between Arctic foxes through the analysis of unique infectious contact rates per rabid individual.

2.2.2. Entities, state variables and scales

The ABM integrates two layers representing the landscape and simulated Arctic foxes. Two types of entities are thus included in the model: landscape cells and Arctic foxes that are modelled as mobile individuals occupying the cells. State variables associated with each entity are either static (fixed during a given simulation) or dynamic (updated at each time step), and are listed in Table 1.

As experiments involving a range of large landscapes with controlled spatial distribution of resources are often difficult to carry out and replicate, we generated a set of theoretical landscapes varying in spatial

Table 1
List of entities and their associated state variables used in the ABM. The type and description of the state variables, as well as the process in which the state variable is updated at each time step, are mentioned.

Entity	Type of state variable	Description of state variable (unit)	Process in which the state variable is updated
Landscape cell	Static	Unique ID number	
		Location (x, y) of the centroid (km)	
		Resource availability (G) (0 – 1)	
Arctic foxes	Static	Unique ID number	
		Location (x, y) of the hotspot (i.e., resource-rich area) for migrating and dispersing individuals (km)	
		Movement strategy (migration, dispersal, nomadism, or sedentarism)	
		Incubation period (day)	
		Infectious period (day)	
		Probability of transmitting rabies according to the aggressive or dumb form of the virus (0 – 1)	
		Probability of becoming infected (i.e., exposed to rabies but not yet infectious) through direct contact with an infectious individual (0 – 1)	
	Dynamic	Location (x, y) of the current cell (km)	Arctic fox movement
		Movement phase (emigration or transfer)	Arctic fox movement
		Movement state (rest, outbound, search, forage, or inbound)	Arctic fox movement
		Probability of leaving the natal cell (or den) (0 – 1)	Arctic fox movement
		Cumulative number of movement steps during the transfer phase	Arctic fox movement
		Health state (uninfected, exposed, or infectious)	Rabies transmission
		Time since exposure to rabies (hour)	Rabies transmission
		Time since the onset of rabies symptoms (hour)	Rabies transmission

aggregation (clustering) of resources from mean-zero and variance-one Gaussian random fields (GRFs) with an exponential covariance function (Fig. B.1 in Appendix B), similarly to Forester et al. (2009). We assumed that there is no nugget effect. GRFs have been used in several studies to model the spatial dependence of ecological processes, such as animal movement (e.g., Aarts et al., 2013; Bracis et al., 2015; Dupont et al., 2021). Our theoretical landscapes consisted of a grid of 700 (rows) × 700 (columns) cells with a cell resolution of 1 km, which represents an area of 490,000 km^2. The scale parameter ϕ_G that controls the level of autocorrelation between the grid cells varied from 10 to 250 ($\phi_G = 10$, 25, 50, 150, and 250). High values of ϕ_G generate landscapes composed of highly aggregated resources, while at low values of ϕ_G, resources are randomly distributed in the landscape. To improve the visual interpretation of the resulting resource gradient, the GRF values were scaled between 0 and 1 using a linear stretch method (Johnson et al., 2004) that takes the form:

$$G(\mathrm{x}) = \frac{w(\mathrm{x}) - w_{\min}}{w_{\max} - w_{\min}}$$

The term $w(\mathrm{x})$ represents the GRF values at each location $\mathrm{x} = (x, y)$ in the landscape, and $w_{\min}$ and $w_{\max}$ correspond to the smallest and highest GRF values, respectively. The values of G can be interpreted as estimating the probability that the spatial location is in a resource-rich area (Tardy et al., 2021). For each landscape, we identified hotspots as areas of high resource availability where the values of G were above a threshold value (HT_G), which varied from 0.6 to 0.8. High values of HT_G reduce the number of hotspots in the landscape. The center of each hotspot was defined as the location with the highest value of G (Lai et al., 2015).

The ABM runs at discrete time steps of one hour.

2.2.3. Process overview and scheduling

The Arctic fox layer depends on the landscape layer based on two ecological processes that are described in the subsection "Submodels": 1) Arctic fox movement and 2) rabies transmission. The ABM evolves in a cell-based setting (Bian, 2003) in which the ecological processes act at the cell scale. Consequently, the context-dependencies (i.e., conspecific density and resource availability) operating in the movement process act at this scale. Fox individuals that are present in a given cell define a distinct open population (i.e., experiencing recruitment through immigrations, or losses through deaths and emigrations). For simplicity, we assumed that the populations of simulated Arctic foxes were geographically closed (i.e., no death, immigration, or emigration from outside the landscape). All simulations were performed over a total period of 5000 h (~ 208 days), which corresponds to the sea ice period (October 25 – May 31). At each time step, each simulated Arctic fox can move to another cell according to movement rules that are defined from HMMs. Once individual locations are updated, rabies transmission success is evaluated between a susceptible fox and an infectious fox (Fig. 1). The simulation ends when the maximum number of steps is reached (i.e., 5000 steps) to avoid having simulated Arctic foxes moving all the time within the landscape.

2.2.4. Design concepts

The current version of the ABM does not include collectives.

Basic principles: Given the ability of Arctic foxes to detect food resources on sea ice (Lai et al., 2015), the ABM integrates a foraging movement process that involves two phases, emigration from the den and transfer towards a hotspot, in which context-dependencies operate at the cell scale. The foraging trip during the transfer phase is modelled using HMMs that segment movement trajectories into different behavioral states based on time series of step lengths and turning angles (Langrock et al., 2012; Zucchini et al., 2017). Most input parameters of the simulated HMMs were estimated from satellite-tracked Arctic fox location data associated with four movement strategies (i.e., migration, dispersal, nomadism, and sedentarism; see the subsection "Characterization of broad-scale movement strategies" in the section "Results"). The HMMs were used to calculate state-switching probabilities as a function of covariates, which allows modulating behavioral decisions of Arctic foxes in response to environmental conditions. The ABM thus differs from other Arctic rabies models (Moran et al., 2021, 2022; Simon et al., 2019) in that our model explicitly describes Arctic fox movement behavior and its interaction with the environment.

Emergence: The simulated movement patterns associated with the four strategies (i.e., migration, dispersal, nomadism, and sedentarism) are affected by landscape characteristics. Combined with stochasticity in the movement process, this leads to the emergence of heterogeneous spatial distribution patterns among simulated Arctic foxes, giving rise to spatial heterogeneity in contact rates between individuals.

Adaptation: During the emigration phase, simulated Arctic foxes decide to leave their natal cell (or den) based on the number of conspecifics within the cell. The probability of emigrating from the natal cell increases with increasing conspecific abundance. When an Arctic fox emigrates, the individual enters the transfer phase and moves to a landscape cell determined by the hidden Markov state process. The latter is simulated at each time step from an estimated state transition probability matrix. The probabilities of transitioning from one state to another depend on three covariates: distance from the current location to a hotspot, the time since departure from the den (or natal cell), and resource availability (see the subsection "Submodels" for more details on the movement process).

Objectives: Simulated Arctic foxes move towards foraging areas within the landscape. Based on the sequences of foraging trips observed in satellite-tracked Arctic foxes, the movement trajectories of simulated foxes reflect a fitness-seeking behavior, with a larger amount of time spent in foraging rather than resource-searching behavior (see the subsection "State sequences of foraging trips" in the section "Results"). Individuals can be constrained to forage in close proximity or away from their natal cell (or den), depending upon the hotspot locations.

Learning: Simulated Arctic foxes change their behavior over time as a function of their previous experiences. These changes were modelled through simulated HMMs in which the behavioral state process has a Markov property, such that the future state depends on the current state, with the aim of predicting future movement. Fitted HMMs that were used to parameterize the simulated HMMs were applied in an unsupervised learning context to infer behavioral states from movement data. In an unsupervised learning context, behavioral state classification is based on step length and turning angle distributions, and is not validated by direct observations of behaviors.

Prediction: In the simulated HMMs of the ABM, the behavioral state process that is characterized by a transition probability matrix predicts the future state of simulated Arctic foxes, given their current state. The choice of the next cell thus relies on the previous experience with the objective for foxes to reach a hotspot or return to their den after a certain period of time. More information on the behavioral state process is given in the subsection "Submodels".

Sensing: Simulated Arctic foxes have knowledge of conspecific density and habitat quality in their natal cell. Individuals move according to what they perceive in the landscape and can detect the presence of hotspots within their perceptual range.

Interaction: Intraspecific competition for resources is implicitly modelled in the ABM. Density dependence in the emigration process operates at the cell scale where the presence of conspecifics is used as a cue for habitat quality. Individuals are more likely to leave their natal cell (or den) when conspecific density is high in the cell.

Stochasticity: The theoretical landscapes are generated from GRFs, which gives rise to stochasticity in the spatial distribution of resources. Some ABM input parameters are drawn from probability distributions (Table 2). Stochasticity is also introduced into the ABM through the Arctic fox movement and rabies transmission processes where the occurrence of an emigration or transmission event is determined by a Bernoulli trial. Finally, the HMMs used in the Arctic fox movement

Table 2
Description of input parameters that are included in the ABM.

Symbol	Description	Range for the sensitivity analysis				References
Category: landscape						
ϕ_G	Level of autocorrelation between the landscape cells	10, 25, 50, 150, 250				
H_G	Threshold value to define a hotspot	[0.6, 0.8]				Calibrated
Category: Arctic fox carrying capacity						
K	Carrying capacity of Arctic foxes in the landscape cells $(/\mathrm{km}^2)$	[0.02, 0.1]				(Angerbjorn et al., 1999)
Category: Arctic fox movement						
μ_i	Mean of the gamma distribution for the step lengths (km/hour) in state i (i = O for "outbound" state, i = S for "search" state, i = F for "forage" state, and i = I for "inbound" state)	Migration μ_O: [2, 3] μ_S: [1.542, 2.125] μ_F: [0.083, 0.167] μ_I: [2.042, 2.875]	Dispersal μ_O: [2.083, 2.708] μ_S: [1.208, 2.125] μ_F: [0.167, 0.250]	Nomadism μ_S: [0.500, 0.667] μ_F: [0.083, 0.096]	Sedentarism μ_S: [0.238, 0.271] μ_F: [0.075, 0.079]	Estimated
σ_i	Standard deviation of the gamma distribution for the step lengths (km/hour) in state i (i = O for "outbound" state, i = S for "search" state, i = F for "forage" state, and i = I for "inbound" state)	σ_O: [0.875, 1.708] σ_S: [0.833, 1.333] σ_F: [0.083, 0.167] σ_I: [0.875, 1.542]	σ_O: [1.042, 1.542] σ_S: [0.792, 1.375] σ_F: [0.125, 0.208]	σ_S: [0.500, 0.625] σ_F: [0.067, 0.079]	σ_S: [0.383, 0.438] σ_F: [0.054, 0.058]	Estimated
κ_i	Concentration of the von Mises distribution for the turning angles (radian) in state i (i = O for "outbound" state, i = S for "search" state, i = F for "forage" state, and i = I for "inbound" state)	κ_O: [1.3, 4] κ_S: [0.6, 1.4] κ_F: [10^{-7}, 0.1] κ_I: [0.3, 1.5] NB: the values are on a logarithmic scale	κ_O: [2.2, 4] κ_S: [1, 2.3] κ_F: [0.4, 0.9] NB: the values are on a logarithmic scale	κ_S: [10^{-7}, 0.1] κ_F: [10^{-7}, 0.1]	κ_S: [10^{-7}, 0.1] κ_F: [10^{-7}, 0.1]	Estimated
β_k^{ij}	Regression coefficients for the transition probabilities from state i to state j as a function of covariates k (i,j = O for "outbound" state, i,j = S for "search" state, i,j = F for "forage" state, i,j = I for "inbound" state, k = G for resource availability, $k = D_t$ for distance to hotspot at time t, and $k = t - t_0$ for time since departure from den)	β_0^{OS}: [3, 5] $\beta_{D_t}^{OS}$: [−5, −1] β_0^{SF}: [−15, −12] β_G^{SF}: [16, 24] β_0^{SI}: [−4, −2] $\beta_{t-t_0}^{SI}$: [2, 10] β_0^{FS}: [12, 15] β_G^{FS}: [−24, −16]	β_0^{OS}: [3, 5] $\beta_{D_t}^{OS}$: [−5, −1] β_0^{SF}: [−15, −12] β_G^{SF}: [16, 24] β_0^{FS}: [12, 15] β_G^{FS}: [−24, −16]	β_0^{SF}: [−15, −12] β_G^{SF}: [16, 24] β_0^{FS}: [12, 15] β_G^{FS}: [−24, −16]	β_0^{SF}: [−15, −12] β_G^{SF}: [16, 24] β_0^{FS}: [12, 15] β_G^{FS}: [−24, −16]	Estimated or calibrated
$DMax_E$	Maximum emigration probability	[0.4, 1]				(Bocedi et al., 2014)
b_E	Inflection point of the density-dependent emigration function	[0.5, 1.5]				(Bocedi et al., 2014)
a_E	Slope at the inflection point of the density-dependent emigration function	[0, 10]				(Bocedi et al., 2014)
Category: rabies transmission						
η_R	Rabies prevalence among Arctic foxes (0 –1)			[0.007, 0.75]	(Mørk and Prestrud, 2004; Rausch, 1972)	
υ	Incubation period of rabies in Arctic foxes (day)			$gamma\left(\text{shape} = \frac{\mu_\upsilon^2}{\sigma_\upsilon}, \text{scale} = \frac{\sigma_\upsilon}{\mu_\upsilon}\right)$, where μ_υ and σ_υ are the mean and standard deviation of the gamma distribution, respectively $\mu_\upsilon : [8{,}180]$, $\sigma_\upsilon = 0.01$	(Mørk and Prestrud, 2004; Rausch, 1972)	
γ	Infectious period of rabies in Arctic foxes (day)			$gamma\left(\text{shape} = \frac{\mu_\gamma^2}{\sigma_\gamma}, \text{scale} = \frac{\sigma_\gamma}{\mu_\gamma}\right)$, where μ_γ and σ_γ are the mean and standard deviation of the gamma distribution, respectively $\mu_\gamma : [1,7]$, $\sigma_\gamma = 0.01$	(Rausch, 1972)	
ρ_c	Probability of rabies transmission among Arctic foxes displaying behavior c when infectious ($c = A$ for "furious" behavior and $c = D$ for "dumb" behavior)			ρ_A: [0.7, 0.9] ρ_D: [0.1, 0.3]	Assumed	
ω_c	Weight for the probability of rabies transmission among Arctic foxes displaying behavior c when infectious ($c = A$ for "furious" behavior and $c = D$ for "dumb" behavior)			ω_A: [0, 1] $\omega_D = 1 - \omega_A$	Assumed	
ε	Probability of encountering conspecifics			[0.2, 0.8]	Assumed	

process are stochastic models where each behavioral state is defined by a random walk (see the subsection "Submodels" for more details on the simulated HMMs).

Observation: All dynamic state variables of each simulated Arctic fox are saved at the end of each time step. In particular, the location of the current cell, the health state and the success of rabies transmission are used to calculate the number of cumulative and unique contacts for each Arctic fox, as well as the number of unique infectious contacts for each rabid individual within a given cell at each time step. The average number of different contacts is saved after each simulation. Given that contacts can be distributed in different ways among individuals (Tardy et al., 2018) (e.g., five contacts for a given individual can be distributed as either five contacts with one conspecific or one contact with five different conspecifics), we calculated the average number of cumulative contacts per Arctic fox (i.e., the average number of conspecifics that have been in direct contact with a simulated fox) and the average number of unique contacts per Arctic fox (i.e., the average number of different conspecifics that have been in direct contact with a simulated fox). We also computed the average number of unique infectious contacts per rabid Arctic fox (i.e., the average number of different conspecifics that have been exposed to rabies following a direct contact with a simulated infectious fox). These metrics provide different information about contact events. Cumulative contact rates influence the probability of transmitting or contracting pathogens, whereas unique contact rates inform on the risk of super-spreading events (Tardy et al., 2018). A direct contact between two simulated Arctic foxes occurred when both foxes were present in the same cell at a given time. Finally, we calculated the proportion of time spent in each behavioral state characterizing the simulated foraging trip of each migrating, dispersing, nomadic or sedentary Arctic fox using the Viberti algorithm (see the subsection "Model parameterization" for more details). The average proportion of time spent in each state is saved after each simulation.

2.2.5. Initialization

Uninfected foxes are randomly distributed in the landscape cells with a number of individuals equal to K at least 100 cells apart from study area boundaries to avoid edge effects. We modelled rabies transmission dynamics by allowing a proportion of infectious foxes (η_R) to transmit the virus to their conspecifics. Infectious foxes displayed either a dumb or furious behavior (see the subsection "Submodels" for more details on the rabies transmission process"). The landscape cells in which each fox is located at the initial time are defined as natal cells (or dens). A hotspot was randomly assigned to each migrating and dispersing Arctic fox. The ABM does not use input data to represent time-varying processes.

2.2.6. Submodels

In the ABM, we integrated two submodels corresponding to two ecological processes: Arctic fox movement and rabies transmission.

Arctic fox movement: Each Arctic fox has a probability of leaving its natal cell (or den) at a given time step t and this probability depends on the presence of conspecifics in the cell. The emigration probability (P_E) is given by the following function introduced by Kun and Scheuring (2006):

$$P_E = \frac{DMax_E}{1 + e^{-\left(\frac{N_{i,t}}{K_i} - b_E\right) a_E}},$$

where $N_{i,t}$ represents the number of simulated Arctic foxes in cell i at time t, K_i corresponds to the carrying capacity of foxes in cell i, and $DMax_E$ is the maximum emigration probability. The parameters b_E and a_E define the inflection point of the density-dependent emigration function and the slope at the inflection point of the function, respectively. A Bernoulli trial determines if the Arctic fox emigrates or not from its natal cell. When the simulated fox does not emigrate from its natal cell, i.e. when $Bern(P_E) = 0$, the fox stays in its natal cell and assumes a resting state.

In the case where the fox emigrates from its natal cell, i.e. when $Bern(P_E) = 1$, we simulated fox movement from HMMs whose most input parameters were estimated by fitting HMMs to Argos-derived locations of Arctic foxes having movement patterns indicative of four movement strategies (i.e., migration, dispersal, nomadism, and sedentarism) (Table 2). Full details on the telemetry location data can be found in the subsection "Model parameterization". We assumed that the trajectories of migrating foxes consisted of four behavioral states (*sensu* Michelot et al., 2017): (1) "outbound" state (O) where movement is fast and highly directed from a den (or natal cell) to a resource-rich area (or hotspot), (2) "search" state (S) where movement is moderately fast with some directional persistence near the hotspot, (3) "forage" state (F) where movement is slow and non-directed within the hotspot, and (4) "inbound" state (or return; I) where movement is fast and highly directed from the hotspot to the den (Fig. 2). For Arctic foxes displaying a dispersal strategy, we considered three states to distinguish "outbound", "search" and "forage" behaviors without a return trip towards the den (Fig. 2). Finally, we assumed that foxes in nomadic and sedentary movement strategies alternated between "search" and "forage" states, and these strategies differed in terms of step lengths and turning angles with more concentrated movements around the den for the sedentary behavior (Fig. 2). The Arctic fox movement in the "search" and "forage" states was modelled using correlated random walks (CRWs) where turning angles were drawn from a von Mises distribution with mean λ and concentration κ. Large κ values imply low variance of the von Mises distribution and, consequently, high directional persistence. We modelled the fox movement in the "outbound" and "inbound" states using biased random walks (BRWs) with attraction towards either the hotspot in the "outbound" state or the den in the "inbound" state by assuming that turning angles followed a von Mises distribution with mean ϕ_t and concentration κ, where $\phi_t = \arctan\left(\frac{y_p - y_t}{x_p - x_t}\right)$ is the direction of the vector pointing from the current location (x_t, y_t) to a focal point (x_p, y_p), i.e. the hotspot or den. For each state, we used a gamma distribution to draw step lengths.

We used a non-observable (hidden) state process ($S_t \in \{O, S, F, I\}$) to describe state-switching dynamics. The state process is governed by a first-order Markov chain and, when combined with the observation process in which the behavioral states are modelled by the types of random walks conditional on the current state, defines a hidden Markov model (Zucchini et al., 2017) for Arctic fox movement. Assuming that the occurrence of a future state at time $t+1$ depends on the current state at time t, the state process S_t was characterized by transition probabilities as follows:

$$\Gamma = \begin{pmatrix} \gamma_{OO} & \gamma_{OS} & 0 & 0 \\ 0 & \gamma_{SS} & \gamma_{SF} & \gamma_{SI} \\ 0 & \gamma_{FS} & \gamma_{FF} & 0 \\ 0 & 0 & 0 & \gamma_{II} \end{pmatrix}, \text{ where } \gamma_{ij} = \Pr(S_{t+1} = j | S_t = i) \text{ for } i, j \in \{O, S, F, I\}$$

The probabilities that are non-zero allow the process to switch from one state to another state. We prevented some transitions by setting probabilities to zero. The matrix Γ was adjusted according to each movement strategy (e.g., the matrix Γ considered above corresponds to the migration strategy). The transition probabilities were expressed as a function of three covariates: (i) distance from the current location to a hotspot at time t (D_t) to model the fact that migrating or dispersing foxes make fast and directed movements away from their den, and tend to switch into other movement states once they reach a hotspot, (ii) the time since departure from the den ($t - t_0$) to model the return towards the den, and (iii) resource availability (G) in the landscape to integrate another key aspect of foraging behavior whereby individuals tend to switch from a searching state to a foraging state with increasing resource availability, with tortuous and shorter movements in resource-rich areas compared to resource-poor areas. The covariate D_t influenced the probability of switching from the "outbound" state to the "search" state

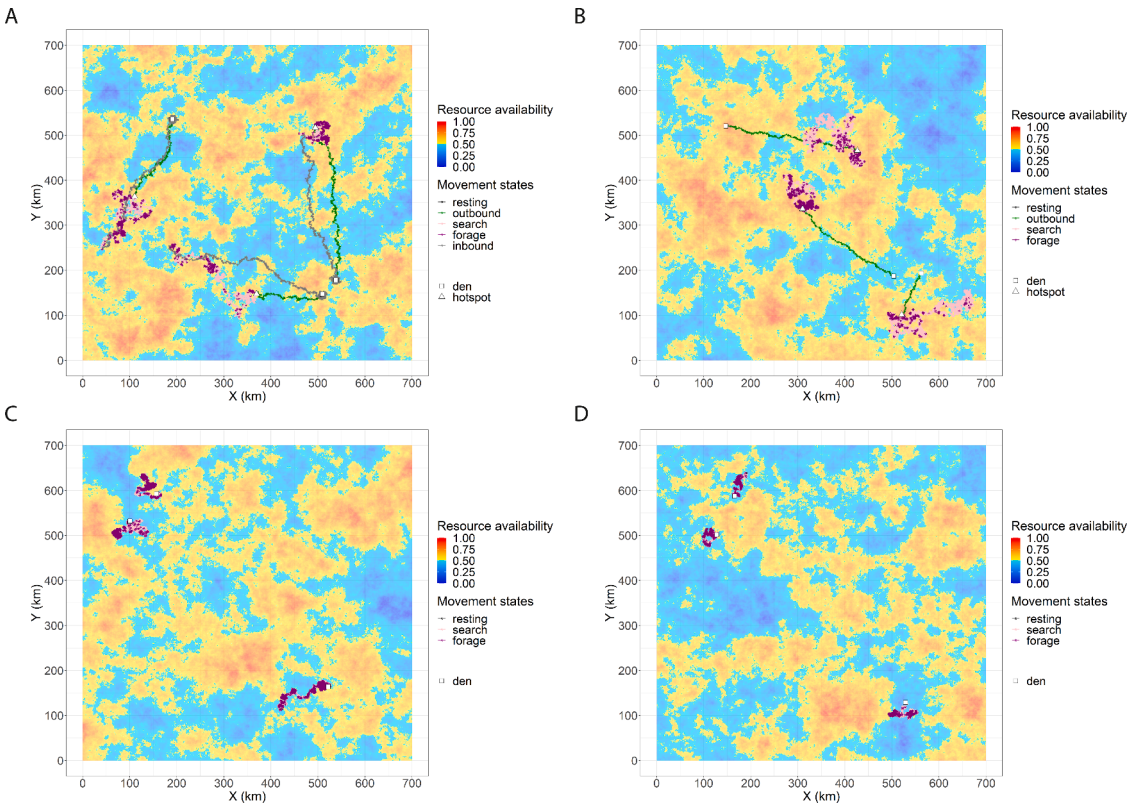

Fig. 2. Examples of foraging trips of three simulated Arctic foxes. Movement trajectories of Arctic foxes having migration-type strategy (A), dispersal-type strategy (B), nomadism-type strategy (C) and sedentarism-type strategy (D) are shown. The four colours correspond to the most probable behavioral states that were decoded with the Viterbi algorithm. White squares indicate dens and white triangles define hotspots (or resource-rich areas).

(γ_{OS}) as follows:

$$\gamma_{OS} = \frac{e^{\eta_{OS}}}{1 + e^{\eta_{OS}}}, \text{ where } \eta_{OS} = \beta_0^{os} + \beta_{D_t}^{os} \times D_t$$

The covariate $t - t_0$ affected the probability of switching from the "search" state to the "inbound" state (γ_{SI}). As there are several non-zero probabilities from the "search" state (i.e., γ_{SF} and γ_{SI}), the transition probability γ_{SI} depended on the covariate $t - t_0$ through a multinomial logit link as follows:

$$\gamma_{SI} = \frac{e^{\eta_{SI}}}{1 + e^{\eta_{SF}} + e^{\eta_{SI}}}, \text{ where } \eta_{SI} = \beta_0^{SI} + \beta_{t-t_0}^{SI} \times (t - t_0)$$

The values of G that were considered fixed over time influenced the probabilities of switching from the "search" state to the "forage" state (γ_{SF}) and from the "forage" state to the "search" state (γ_{FS}) as follows:

$$\gamma_{SF} = \frac{e^{\eta_{SF}}}{1 + e^{\eta_{SF}} + e^{\eta_{SI}}} \text{ and } \gamma_{FS} = \frac{e^{\eta_{FS}}}{1 + e^{\eta_{FS}}}, \text{ where } \eta_{SF} = \beta_0^{SF} + \beta_G^{SF} \times G \text{ and } \eta_{FS} = \beta_0^{FS} + \beta_G^{FS} \times G$$

The parameters β_0^{os}, $\beta_{D_t}^{os}$, β_0^{SI} and $\beta_{t-t_0}^{SI}$, as well as the parameters for the step length and turning angle distributions, were estimated from the Argos-derived location data (see the subsection "Model parameterization" for further details on the fitted HMMs). For example, this results in eight parameters for the gamma-distributed steps and six parameters for the von Mises-distributed angles to estimate in the observation process of the four-state HMMs associated with the migration strategy (Table 2). The mean parameters of turning angles for the "outbound" and "inbound" states were fixed to a large positive number (i.e., 100) to define the bias towards the hotspot or den (McClintock and Michelot, 2018). Due to constraints of environmental data availability, the range of possible values for the input parameters associated with the transition probabilities depending on the value of G (i.e., β_0^{SF}, β_G^{SF}, β_0^{FS}, and β_G^{FS}) was chosen via a simple trial-and-error calibration procedure because precision was not necessary to evaluate the effects of movement strategies on contact rates among simulated Arctic foxes. The remaining elements of the transition probability matrix were obtained so that the rows of the matrix sum to one, and thus varied with time. The fitted HMM parameters were converted into hourly values to parameterize the simulated HMMs of the ABM. A simulated foraging trip started in the "outbound" state for the migration- and dispersal-type movement strategies, and in the "search" state for the nomadism- and sedentarism-type strategies. At each time step, the state process was simulated from the estimated transition probabilities, and a turning angle and a step length were then simulated from the estimated von Mises and gamma distributions, respectively.

Rabies transmission: Rabies transmission events are evaluated at each time step. Virus transmission, which requires direct contact, could occur between simulated Arctic foxes when a susceptible fox (i.e., unexposed to rabies) and an infectious fox shared the same cell during the same time step. The probability that a susceptible fox becomes infected (i.e., exposed to the virus, but not yet infectious) was defined by:

$$P_{RT} = 1 - (1 - \rho_c)^{\varepsilon I_{i,t}},$$

where $I_{i,t}$ represents the number of infectious foxes in the same cell i at time t, ρ_c corresponds to the rabies transmission probability, and ε defines the probability of encountering conspecifics. A Bernoulli trial determines the success of rabies transmission. We varied the rabies transmission probability (ρ_c) according to behavioral changes from rabies infection (i.e., furious when the animal is dominated by aggressive behavior or dumb when the animal is characterized by increased paralysis) (Mørk and Prestrud, 2004). The rabies transmission probability between a susceptible fox and a rabid fox increased when rabid foxes displayed aggressive behavior, whereas the transmission probability decreased when rabid foxes had dumb behavior. In the ABM,

exposed Arctic foxes became infectious after an incubation period (υ). Given that high virulence of rabies contributes to very low levels of natural immunity (Blancou et al., 2009) and serological surveys of Arctic fox populations are rare (but see Ballard et al., 2001 for an example), we supposed that rabies was 100% lethal after an infectious period (γ), similarly to Moran et al. (2021). The incubation and infectious periods were simulated from an Erlang distribution (i.e., gamma distribution with an integer shape parameter) (Krylova and Earn, 2013).

2.3. Model parameterization

The ABM input parameters associated with Arctic fox carrying capacity and rabies transmission were defined from empirical and modeling studies on the Arctic fox and rabies virus. Most input parameters related to the Arctic fox movement process were estimated by fitting HMMs to satellite-tracked Arctic fox location data. In total, 41 adult Arctic foxes were initially captured on Bylot Island, Nunavut, Canada, from 2009 to 2014 and were tracked with Argos satellite collars that were programmed to transmit daily locations during one year. Raw satellite data were filtered and one location per day per individual was kept based on the smallest location error. Details on the capture procedure and telemetry data, including duty cycles and filtering, are given in Lai et al. (2017). We estimated missing daily locations (9.31% of total locations) using continuous-time correlated random walk models as described in Johnson et al. (2008) to reduce uncertainty inherent to movement data. For our analyses, we selected movement records that encompassed one complete winter season corresponding to the sea ice period (October 25 – May 31) (Table A.1 in Appendix A). The sea ice period is of particular interest to explore various movement behaviors of Arctic foxes (Tarroux et al., 2010). Before performing the fitting of HMMs, we removed highly stationary location data based on one-dimensional time series plots of the locations, given that these data give little information and can increase numerical instability (Michelot et al., 2017). For the process of fitting HMMs to the telemetry location data, a cluster analysis was performed using migrating and dispersing Arctic fox locations to identify hotspot centroids. We used the TADPole clustering algorithm implemented in the *dtwclust* package (version 5.5.10; Sardá-Espinosa, 2019) in R and based on 10 clusters, a cutoff distance of 1500 m, and a window size of 1 day. Each cluster was visualized for all individuals and we selected one cluster for each individual to reflect the location of key activity centers. HMM goodness-of-fit was evaluated for each movement strategy (i.e., migration, dispersal, nomadism, and sedentarism) by checking the normality and temporal independence of pseudo-residuals for step lengths and turning angles. For simplicity and as explaining individual variation in transition probabilities was not our central goal, we modelled the behavioral states of all individuals combined without considering individual-level random effects in the HMMs (McClintock, 2021). The HMM fitting to the telemetry data was performed with the *momentuHMM* package (version 1.5.1; McClintock and Michelot, 2018) in R. In this package, the Viterbi algorithm is used to determine the most likely sequence of behavioral states (Zucchini et al., 2017), and the HMM parameters are estimated by likelihood maximization using a recursive algorithm (called the forward algorithm, Zucchini et al., 2017), which requires the specification of "good" starting values for step lengths and turning angles. Following the recommendations of Michelot et al. (2016), we fitted HMMs with several sets of starting values ($N = 50$) that were generated from a uniform distribution, and we selected the best-fitting HMM with the largest likelihood.

2.4. Sensitivity analysis

We performed a global sensitivity analysis (SA) to evaluate the sensitivity of Arctic fox contact patterns to variations in ABM input parameters. A total of 14 input parameters were included in the SA (Table 2): level of autocorrelation between the landscape grid cells (ϕ_G), threshold value to define a hotspot (H_G), carrying capacity of Arctic foxes (K), large-scale movement strategy type (i.e., migration, dispersal, nomadism, and sedentarism) (MS), maximum emigration probability ($DMax_E$), inflection point of the density-dependent emigration function (b_E), slope at the inflection point of the density-dependent emigration function (a_E), rabies prevalence among Arctic foxes (η_R), incubation period of rabies in Arctic foxes (υ), infectious period of rabies in Arctic foxes (γ), probability of rabies transmission among Arctic foxes having the furious form of the virus (ρ_A), probability of rabies transmission among Arctic foxes having the dumb form of the virus (ρ_D), weight for the probability of rabies transmission among Arctic foxes having the furious form of the virus (ω_A), and probability of encountering conspecifics (ε). We used a Latin hypercube sampling scheme to sample 150 different parameter combinations from a uniform probability distribution, satisfying the minimum value of $\frac{4N}{3}$, where N is the number of input parameters (McKay et al., 1979). Because our ABM included stochasticity in the spatial distribution of resources due to the stochastic algorithm of GRFs, we generated 10 replicated landscapes for each parameter combination, resulting in a total of 1500 simulations.

Similarly to our previous papers (Tardy et al., 2021, 2022), we built boosted regression tree (BRT) models (Elith et al., 2008) to assess the relative contribution of each input parameter in predicting ABM output variables, and to identify which of the parameters had the highest effect on these output variables. We used the average number of cumulative contacts per Arctic fox, the average number of unique contacts per Arctic fox, and the average number of unique infectious contacts per rabid Arctic fox as output variables. A Gaussian error structure was used for the loss function of the BRT models. The contact rates were log-transformed in the BRT models to achieve variance homogeneity and to obtain Gaussian error distributions. We tested several combinations of learning rate (0.01, 0.005, 0.001), tree complexity (1 – 5) and bag fraction (0.5, 0.7, 0.9) to determine optimal settings for the BRT models. We selected the parameter combination with the lowest 10-fold cross-validation deviance to fit the final BRT model. We also evaluated the relative contribution of the input parameters based on their effect on the ecological processes that are implemented in the ABM. The input parameters belonged to four categories: landscape, carrying capacity of Arctic foxes, Arctic fox movement, and rabies transmission (Table 2). We visualized the relationships between the output variables and the most influential input parameters with partial dependence plots in which 95% confidence intervals were obtained from 500 bootstrap replicates. We tested the significance of the strongest interactions using 100 bootstrap resampling iterations (Pinsky and Byler, 2015). The BRT models were built from the *dismo* (version 1.1.4) and *ggBRT* (version 0.0.0.9000) packages in R (Hijmans et al., 2020; Jouffray et al., 2019).

3. Results

3.1. Broad-scale movement strategies

The analysis of the NSD time-series of Arctic foxes ($N = 41$) using NSD statistics with a latent state model showed inter-individual variations in coarse-scale movement strategies. We found that 66% ($N = 27$) of Arctic foxes were sedentary individuals with probabilities of switching from one movement mode to another of $q_{22} \leq 0.90$ and $q_{33} \leq 0.90$. The results also revealed that 12% ($N = 5$) of foxes had patterns of transition between the modes similar to nomadic strategy ($q_{11} > 0.95$, $q_{22} > 0.90$, and $q_{33} \leq 0.85$), and 12% ($N = 5$) of foxes displayed dispersal behavior ($q_{11} > 0.95$, $q_{22} > 0.95$, and $q_{33} > 0.85$). Finally, 10% ($N = 4$) of foxes showed migration behavior with transition probabilities of $q_{11} > 0.95$, $q_{22} > 0.95$ and $q_{33} > 0.85$, together with the presence of transition back from the second encamped mode. The classification of large-scale movement strategies in Arctic foxes was not sensitive to variation in the starting date of the NSD time-series. On average, overall agreement for the classification of strategies was 91%

(range: 72 – 100%). At the daily level, we found that 82% of monitoring days had > 80% agreement (range: 28 – 100%) among the iterations, and 65% of days had > 95% agreement (range: 9 – 100%).

3.2. State sequences of foraging trips

Given the fitted HMMs for each movement strategy, the analysis of pseudo-residuals for the step lengths and turning angles showed that the pseudo-residuals were approximately normally distributed (Fig. C.1–C.4 in Appendix C). There was some autocorrelation in the pseudo-residuals, in particular for the step lengths from the 2-state HMM fitted to the Argos tracking data of sedentary Arctic foxes (Fig. C.1–C.4 in Appendix C), which can suggest the need for adding more states or covariates. However, model complexity can make biological interpretation of states difficult and lead to unstable parameter estimation (Pohle et al., 2017). Our choice of the number of states was based on the results of the analysis of the NSD time-series using NSD statistics with a latent state model, as well as the ecology of Arctic foxes and the constraints of available environmental data. The fitted HMMs revealed that sedentary Arctic foxes spent 79% of their time foraging (range: 44 – 100%) and 23% of their time searching for resource-rich foraging areas (range: 1 – 56%). Nomadic Arctic foxes were in the foraging state 80% of their time (range: 70 – 91%) and in the searching state 20% of their time (range: 9 – 30%). We found that migrating foxes allocated 39% of their time to foraging behavior (range: 5 – 59%), 25% of their time searching for resource-rich foraging areas (range: 20 – 33%), 21% of their time to the inbound trip from the foraging area (or hotspot) to the den (range: 10 – 45%), and 15% of their time to the outbound trip from the den to the foraging area (range: 5 – 30%). Dispersing foxes were in the outbound trip 41% of their time (range: 3 – 77%), in the foraging state 40% of their time (range: 14 – 83%), and in the searching state 19% of their time (range: 2 – 39%). In addition, the fitted HMMs showed that the transition probabilities from "outbound" to "search" states for Arctic foxes displaying migration and dispersal behaviors decreased with increasing distance to the hotspot. Migrating and dispersing Arctic foxes tended to perform searching activities for resource-rich areas when they were located at less than 400 km from these areas (Fig. 3A and B). Finally, we observed that the transition probabilities from "search" to "inbound" states for Arctic foxes having migration behavior increased when the time since departure from the den was high. Migrating foxes tended to start returning to their den after about 60 days (Fig. 3.C). These patterns were reproduced by the ABM.

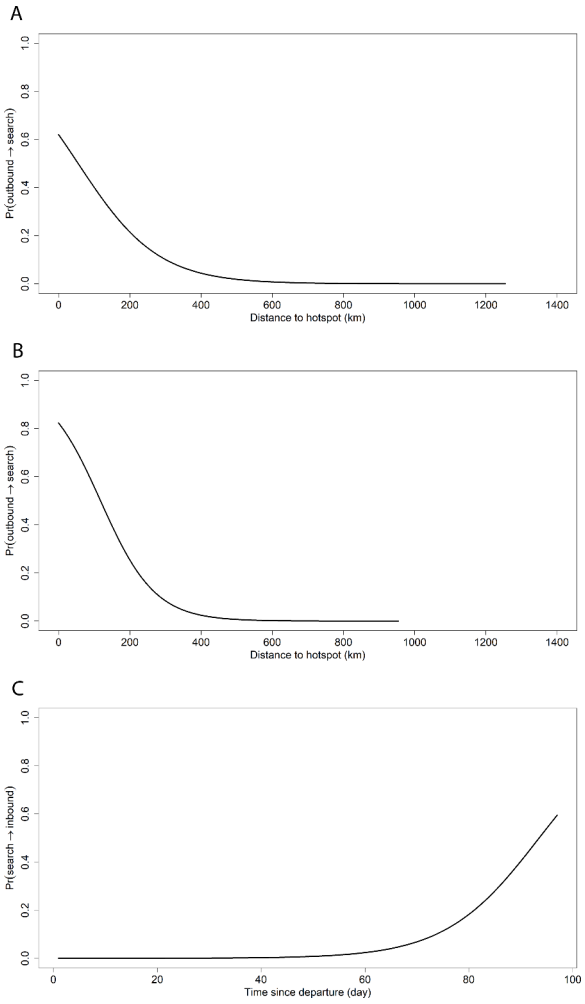

Fig. 3. Transition probabilities between states as a function of time-varying covariates. Plots representing transition probabilities from "outbound" to "search" as a function of distance to hotspot (km) for dispersing Arctic foxes (A), transition probabilities from "outbound" to "search" as a function of distance to hotspot (km) for migrating Arctic foxes (B), and transition probabilities from "search" to "inbound" as a function of time since departure (day) from den for migrating Arctic foxes (C).

3.3. Contact rates among Arctic foxes

The BRT models performed well for quantifying the relative contribution of each ABM input parameter on contact rates among Arctic foxes, with 10-fold cross-validation deviance explained ranging from 82% to 99% and with cross-validated correlation ranging from 0.91 to 0.99 (Table D.1 in Appendix D). In the sections below, we describe the relationships between contact rates among Arctic foxes and the most influential input parameters (≥10% relative influence). The relative influence of each input parameter is provided in Appendix D (Fig. D.1).

The average number of cumulative contacts per Arctic fox was mainly influenced by input parameters associated with rabies transmission dynamics (73% relative influence) and carrying capacity of Arctic foxes (15% relative influence; Table D.2 in Appendix D). The output variable was best predicted by a negative relationship with increasing prevalence of rabies in Arctic foxes (η_R; 63% relative influence; Fig. 4.A). In contrast, a positive relationship was observed for carrying capacity of Arctic foxes in the landscape cells (K; 15% relative influence; Fig. 4.A), meaning that high cumulative contact rates were associated with high Arctic fox densities (range: 0.07 – 0.1 individuals/km^2). The strongest pairwise interaction was high (interaction size: 10.24) and significant ($p < 0.05$), reflecting the interacting effects of the most influential predictors with cumulative contact rates being highest in areas where prevalence of rabies was low and Arctic fox density was high (Fig. D.2 in Appendix D). The other interactions between predictors were weak (interaction size < 3.1).

The average number of unique contacts per Arctic fox was mainly influenced by input parameters associated with rabies transmission dynamics (46% relative influence), Arctic fox movement (36% relative influence), and carrying capacity of Arctic foxes (16% relative influence; Table D.2 in Appendix D). Three predictors contributed most strongly to predicting the output variable: prevalence of rabies in Arctic foxes (η_R; 40% relative influence; negatively correlated), movement strategy type (35% relative influence; sedentarism < nomadism < migration < dispersal), and carrying capacity of Arctic foxes in the landscape cells (K; 16% relative influence; positively correlated; Fig. 4.B). The strongest pairwise interaction was low (interaction size: 3.55) and not significant ($p > 0.05$), reflecting the additive rather than interactive effects of the most influential predictors. A significant difference in unique contact rates was found between migration and dispersal strategies, with higher unique contact rates per individual observed among dispersing Arctic foxes (Fig. 5.A; two-sided pairwise Wilcoxon rank-sum test with Bonferroni correction: $W = 35{,}811$ and $p < 0.0001$). There were also significant differences in unique contact rates between these two strategies

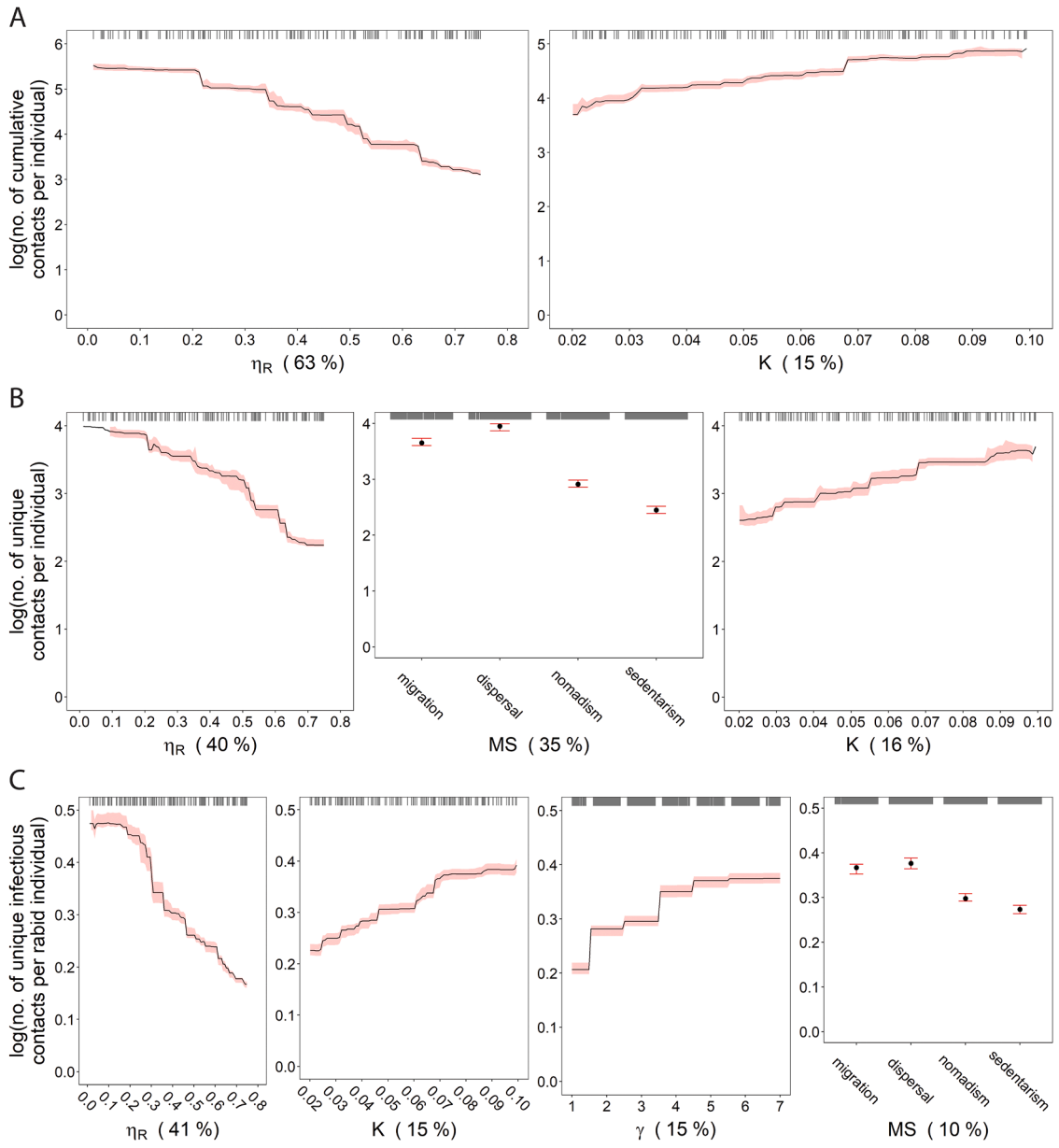

Fig. 4. Relationships between the most influential predictors and contact rates among Arctic foxes. Partial dependency plots with bootstrapped 95% confidence intervals (red) predicting (A) the average number of cumulative contacts per individual, (B) the average number of unique contacts per individual, and (C) the average number of unique infectious contacts per rabid individual. The contact rates were log-transformed. Black tick marks at the top of each plot represent the distribution of raw contact rates across each predictor. Relative influence (%) of the most influential predictors (≥10% relative influence) is shown in parentheses. η_R: prevalence of rabies virus in Arctic foxes; *K*: carrying capacity of Arctic foxes in the landscape cells; *MS*: large-scale movement strategy type (migration, dispersal, nomadism and, sedentarism); γ: infectious period of rabies in Arctic foxes.

and those associated with nomadism- and sedentarism-type movements (Fig. 5.A; two-sided pairwise Wilcoxon rank-sum test with Bonferroni correction: $W = 98{,}641$ and $p < 0.0001$ for migration vs. nomadism, $W = 96{,}195$ and $p < 0.0001$ for migration vs. sedentarism, $W = 119{,}418$ and $p < 0.0001$ for dispersal vs. nomadism, $W = 107{,}179$ and $p < 0.0001$ for dispersal vs. sedentarism, $W = 127{,}573$ and $p < 0.0001$ for nomadism vs. sedentarism). Migrating Arctic foxes displayed higher unique contact rates when they spent <40% of their time in the "outbound" state rather than in the other states (Fig. 6.A; two-sided pairwise Wilcoxon rank-sum test with Bonferroni correction: $W = 21{,}151$ and $p < 0.0001$ for outbound vs. search, $W = 20{,}921$ and $p < 0.0001$ for outbound vs. forage, $W = 20{,}038$ and $p < 0.0001$ for outbound vs. inbound). We observed higher unique contact rates among dispersing Arctic foxes when these foxes allocated <50% of their time in the "outbound" state than in the other states (Fig. 6.B; two-sided pairwise Wilcoxon rank-sum test with Bonferroni correction: $W = 35{,}574$ and $p < 0.0001$ for outbound vs. search, $W = 38{,}460$ and $p < 0.0001$ for outbound vs. forage). Unique contact rates among dispersing Arctic foxes increased when they invested more time in the "search" and "forage" states (>50% of their time) (Fig. 6.B; two-sided pairwise Wilcoxon rank-sum test with Bonferroni correction: $W = 212$ and $p < 0.0001$ for outbound vs. search, $W = 77$ and $p < 0.0001$ for outbound vs. forage, $W = 345$ and $p = 1$ for search vs. forage).

The average number of unique infectious contacts per rabid Arctic fox was mainly influenced by input parameters associated with rabies transmission dynamics (71% relative influence), carrying capacity of Arctic foxes (15% relative influence), and Arctic fox movement (13% relative influence; Table D.2 in Appendix D). A negative relationship

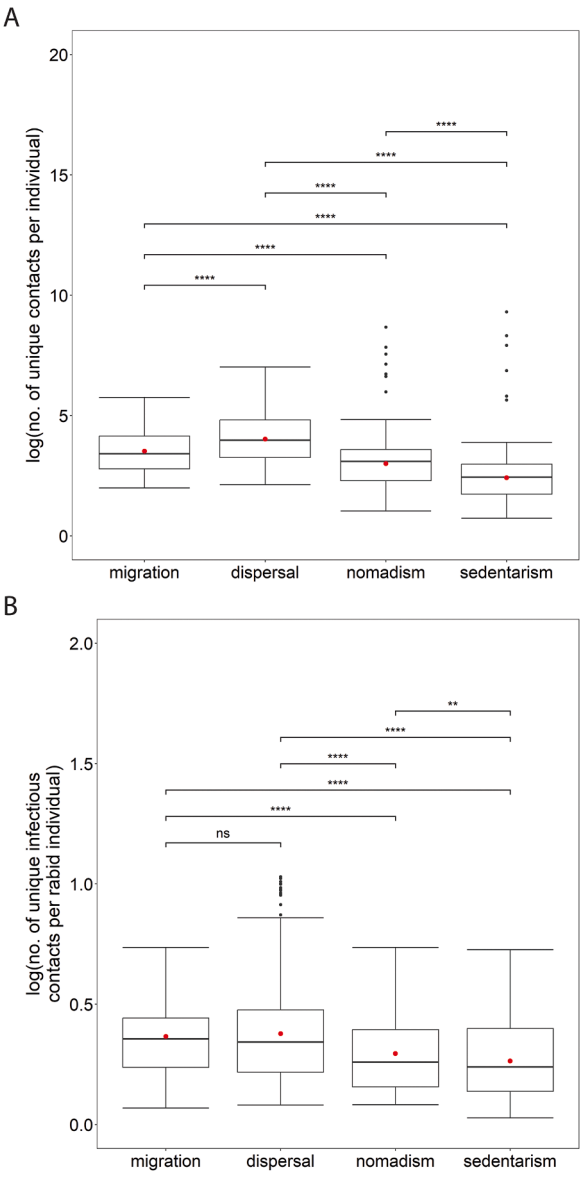

Fig. 5. Distribution of unique contact rates per Arctic fox for each movement strategy. Boxplots represent the distribution of raw values of unique contact rates per Arctic fox (A) and unique infectious contact rates per rabid Arctic fox (B). Horizontal lines indicate the median value of raw data, boxes represent the interquartile range (25th to 75th percentile), vertical lines correspond to ± 1.5 times the interquartile range to the 25th and 75th percentiles. Outliers (i.e., points beyond 1.5 times the interquartile range) are represented by points. All comparisons between states were performed using a two-sided pairwise Wilcoxon rank-sum test with Bonferroni correction. **** $p < 0.0001$; *** $p < 0.001$; ** $p < 0.01$; * $p < 0.05$; ns = not significant.

with increasing prevalence of rabies in Arctic foxes was the main predictor of the output variable (η_R; 41% relative influence; Fig. 4.C). The latter also displayed a positive relationship with increasing carrying capacity of Arctic foxes in the landscape cells (K; 15% relative influence) and with increasing infectious period (γ; 15% relative influence; Fig. 4.C). Finally, the movement strategy type was also an influential predictor of the output variable (10% relative influence; sedentarism < nomadism < migration < dispersal; Fig. 4.C). The strongest pairwise interaction was low (interaction size: 0.58) and not significant ($p > 0.05$), reflecting the additive rather than interactive effects of the most influential predictors. There was no significant difference between migration and dispersal strategies in unique infectious contact patterns among rabid Arctic foxes (Fig. 5.B; two-sided pairwise Wilcoxon rank-sum test with Bonferroni correction: $W = 50{,}879$ and $p = 1$), but significant differences were observed between these strategies and those associated with nomadism- and sedentarism-type movements (Fig. 5.B; two-sided pairwise Wilcoxon rank-sum test with Bonferroni correction: $W = 95{,}945$ and $p < 0.0001$ for migration vs. nomadism, $W = 78{,}568$ and $p < 0.0001$ for migration vs. sedentarism, $W = 93{,}943$ and $p < 0.0001$ for dispersal vs. nomadism, $W = 78{,}841$ and $p < 0.0001$ for dispersal vs. sedentarism, $W = 104{,}262$ and $p = 0.012$ for nomadism vs. sedentarism). Migrating Arctic foxes exhibited higher unique infectious contact rates when they spent <40% of their time in the "outbound" state rather than in the other states (Fig. 6.C; two-sided pairwise Wilcoxon rank-sum test with Bonferroni correction: $W = 22{,}254$ and $p < 0.0001$ for outbound vs. search, $W = 22{,}266$ and $p < 0.0001$ for outbound vs. forage, $W = 20{,}736$ and $p < 0.0001$ for outbound vs. inbound). Unique infectious contact rates among migrating Arctic foxes increased when they invested more time in the "forage" and "inbound" states (>40% of their time) (Fig. 6.C; two-sided pairwise Wilcoxon rank-sum test with Bonferroni correction: $W = 0$ and $p < 0.0001$ for outbound vs. forage, $W = 1230$ and $p < 0.0001$ for outbound vs. inbound, $W = 4$ and $p = 0.036$ for search vs. forage, $W = 95$ and $p = 1$ for search vs. inbound, $W = 200$ and $p = 1$ for forage vs. inbound). We found higher unique infectious contact rates among dispersing Arctic foxes when these foxes spent <50% of their time in the "outbound" state than in the other states (Fig. 6.D; two-sided pairwise Wilcoxon rank-sum test with Bonferroni correction: $W = 33{,}236$ and $p < 0.0001$ for outbound vs. search, $W = 37{,}604$ and $p < 0.0001$ for outbound vs. forage). Dispersing Arctic foxes had a greater chance to become infected following contact with a rabid conspecific when they invested more time in the "forage" state (>50% of their time) (Fig. 6.D; two-sided pairwise Wilcoxon rank-sum test with Bonferroni correction: $W = 0$ and $p < 0.0001$ for outbound vs. forage, $W = 157$ and $p = 0.0008$ for search vs. forage). We tested other correction methods (i.e., Benjamini-Hochberg and Benjamini-Yekutieli) for multiple comparisons using the Wilcoxon rank-sum test, and the results for all contact measures were similar to those obtained with Bonferroni correction.

4. Discussion

Arctic rabies is an enzootic disease in Arctic and sub-Arctic regions, which poses a serious threat to human and animal health (Mørk and Prestrud, 2004). Despite a growing body of literature covering the ecology of Arctic foxes, important knowledge gaps exist regarding the ecology of the Arctic rabies virus, which includes the influence of host behavior on rabies transmission events (Simon et al., 2020). In particular, the ecological processes modulating contact rates among Arctic foxes are often speculative, limiting our understanding of the consequences of environmental changes on rabies dynamics in the Arctic. We built the first spatially explicit agent-based model for Arctic fox rabies in which HMMs were used to mechanistically simulate broad-scale movement strategies (migration, dispersal, nomadism, and sedentarism) in Arctic foxes. Our results showed that rabies transmission dynamics and fox carrying capacity were key predictors of cumulative contact rates among Arctic foxes, while rabies transmission dynamics, fox movement behavior and fox carrying capacity determined unique contact rates.

4.1. Contact patterns in Arctic fox populations

We found differences between cumulative and unique contact rates. Our results revealed that low prevalence of rabies among Arctic foxes (0 – 0.2%) and increased carrying capacities of Arctic foxes (0.07 – 0.1 foxes/km^2) resulted in high cumulative contact rates between Arctic foxes, with an increase in fox home range overlap tending to occur in areas where resources were clustered and scarce (hotspots with resource availability values > 0.78). In our study, low prevalence of rabies allows maintaining Arctic fox populations at high density levels preventing their extinction. Field studies showed that prevalence of rabies was low among Arctic foxes (0.3% – 3%), suggesting that the virus is not endemic

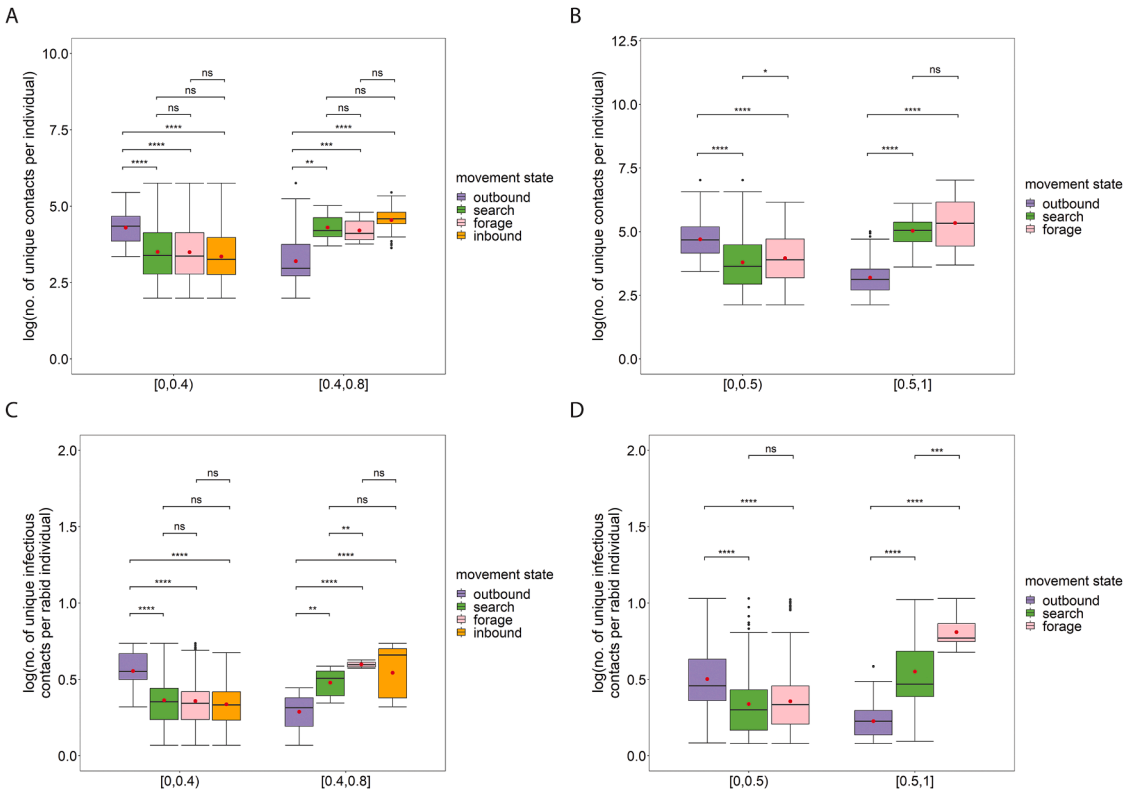

Fig. 6. Distribution of unique contact rates per migrating and dispersing Arctic fox for each movement state according to two levels of proportion of time spent in the states. Boxplots represent the distribution of unique contact rates per migrating Arctic fox (A), unique contact rates per dispersing Arctic fox (B), unique infectious contact rates per migrating rabid Arctic fox (C), and unique infectious contact rates per dispersing rabid Arctic fox (D). Horizontal lines indicate the median value of raw data, boxes represent the interquartile range (25th to 75th percentile), vertical lines correspond to ± 1.5 times the interquartile range to the 25th and 75th percentiles. Outliers (i.e., points beyond 1.5 times the interquartile range) are represented by points. All comparisons between the states were performed using a two-sided pairwise Wilcoxon rank-sum test with Bonferroni correction. **** $p < 0.0001$; *** $p < 0.001$; ** $p < 0.01$; * $p < 0.05$; ns = not significant.

in local Arctic fox populations, but is occasionally introduced by foxes migrating on sea ice (Prestrud et al., 1992). From the ABM simulations, cumulative contact rates increased nonlinearly with Arctic fox density, and tended to saturate at higher individual densities, indicating that rabies transmission among Arctic foxes should be intermediate between density- and frequency-dependent transmission (Smith et al., 2009). The nonlinear nature of the relationship between contact rates and individual density results from changes in state-switching movement dynamics with resource availability. Our results showed a higher relative influence of the landscape on the number of cumulative contacts per fox compared to the number of unique contacts per fox. Landscape heterogeneity can produce scarce hotspots of resources, and resource scarcity can lead to higher Arctic fox densities around scavenged carcasses, and thus create opportunities for pathogen transmission by close contact (Simon et al., 2020). For example, Arctic foxes can congregate in large numbers in resource-rich areas during extraterritorial foraging of adults in winter (December – February), which can increase contact rates between individuals (Lai et al., 2015).

In addition, our results revealed that low prevalence of rabies among Arctic foxes (0 – 0.2%), dispersal-type movement strategy, and increased carrying capacities of Arctic foxes (0.07 – 0.1 foxes/km^2) induced high unique contact rates between Arctic foxes. Using the ABM simulations, we observed that unique contact rates increased among dispersing Arctic foxes when they allocated <50% of their time to the outbound trip, suggesting areas at highest risk for unique contacts between dispersing Arctic foxes are those not too far away from dens. The outbound trip, which is characterized by fast and highly directed movements, occurs when a fox leaves its den to search for new resources. It then follows a transitional phase of searching activity (where movement is moderately fast with some directional persistence near resource-rich areas) between the outbound state and the foraging state (where movement is slow and non-directed within resource-rich areas). Dispersing Arctic foxes investing more time in searching and foraging activities (>50% of their time) were more likely to have contact with different conspecifics. This pattern was also observed for Arctic foxes displaying a migration-type movement strategy (the second at-risk strategy). These foxes exhibited higher unique contact rates when they spent <40% of their time in the outbound state. From the fitted HMMs, migrating and dispersing Arctic foxes tended to engage in searching activities for resource-rich areas when they were located less than 400 km from these areas. Despite a large number of studies showing the important role of animal migration in long-distance spread of pathogens (Fritzsche McKay and Hoye, 2016; Risely et al., 2018; Satterfield et al., 2018), the demonstration of the impact of dispersal behavior on pathogen transmission remains limited (Boulinier et al., 2016). Our results suggest that the dispersal-type movement strategy has the potential to act as a super-spreading process as this strategy is likely to increase the number of unique contacts with other conspecifics compared to migration, nomadism and sedentarism behaviors. As observed for migrating host individuals (Teitelbaum et al., 2018), it is expected that dispersing host individuals that visit multiple sites across a broad geographic range would be more likely to be exposed to a high number and diversity of pathogens, owing to increased contacts with other host individuals (Shaw et al., 2018). Arctic foxes can move over long distances outside their home range (Lai et al., 2017; Tarroux et al., 2010). For example, an Arctic fox travelled 4,415 km in four months between Svalbard (Norway) and Ellesmere Island (Canada) (Fuglei and Tarroux, 2019). However, our simulation results suggest that a dispersal strategy over such long distances is not the most critical for Arctic rabies transmission. It has been shown that reduced long-distance movements of hosts could

favor pathogen transmission by increasing host exposure to contaminated habitats where pathogens have accumulated in the environment over time (Hall et al., 2014).

Finally, we found that low prevalence of rabies among Arctic foxes (0 – 0.2%), increased carrying capacities of Arctic foxes (0.07 – 0.1 foxes/km^2), high infectious periods (4 – 7 days), and long-distance movement strategies (i.e., migration and dispersal) led to high unique infectious contact rates from rabid Arctic foxes. Long infectious periods are required to favor infectious contacts and thus to maintain rabies even in populations at high Arctic fox densities. Generally, the infectious period of rabies varies between one and seven days, and Arctic foxes can die between one and three days after the onset of symptoms (Konovalov et al., 1965). No significant difference in unique infectious contact patterns among Arctic foxes was found between migration and dispersal strategies, but these two strategies produced higher unique infectious contact rates compared to nomadism- and sedentarism-type movement strategies. The trend observed in the unique infectious contact patterns among migrating and dispersing Arctic foxes was similar to that found in the unique contact patterns, with migrating and dispersing Arctic foxes displaying higher unique infectious contact rates when they spent <40% and <50% of their time in the outbound trip, respectively, rather than in the other states. Unique infectious contact rates were amplified among dispersing Arctic foxes when they invested more time in foraging activities (>50% of their time), while for migrating Arctic foxes, the chance to become infected after contact with a rabid conspecific increased when they allocated more time in both foraging and inbound trips (>40% of their time). To model the return to the den, the state sequence alternates first with the foraging and searching trips, and finally is forced to remain in the inbound trip until the end of a given simulation. Migrating Arctic foxes increased their time spent in the inbound trip when they moved across several foraging areas, and tended to cross previously visited areas in order to return to their den. This can produce contact events with conspecifics that are located close to foraging areas. Our results show that consideration of the allocation of time to behavioral states is important for judging the risk of Arctic rabies transmission. In particular, increased proportion of time engaged in foraging activities that align with reduced long-distance movement strategies is likely to promote infectious contacts. Although several field and modeling studies have shown that the influence of resource availability can produce a large range of disease outcomes in foraging hosts (reviewed in Altizer et al., 2018; Becker et al., 2015), rabies models incorporating behavioral state analysis provide an under-explored avenue for investigating contact dynamics and rabies transmission.

4.2. Implications for Arctic rabies management

Rabies management strategies that are traditionally used to prevent or control rabies virus circulation in wildlife include oral rabies vaccination (ORV), trap-vaccinate-release, population reduction, and fertility control (Elmore et al., 2017; Sterner and Smith, 2006). Our results revealed that contact rates between Arctic foxes increased following a nonlinear saturating function of individual density, suggesting that rabies transmission among Arctic foxes should be intermediate between density- and frequency-dependent transmission. Consequently, reduction in fox density may not be an optimal strategy as rabies transmission among Arctic foxes is not only density-dependent (i.e., contact rates varying linearly with individual density). Rabies management under Arctic conditions represents a challenge. However, ORV has been shown to be effective for eliminating rabies among Arctic foxes, especially when areas containing high densities of foxes (e.g., anthropogenic areas) are targeted for bait distribution (Follmann et al., 2011, 2004). Given that Arctic foxes exhibit a high detection ability of localized food resources such as marine carrion on sea ice (Lai et al., 2015), the use of feeding sites to deliver oral rabies vaccines may thus be an effective strategy on condition of minimizing risks to human and animal health (e.g., exposure to pathogens) (Becker et al., 2015; Civitello et al., 2018; Murray et al., 2016). Murray et al. (2016) recommend to 1) provide nutritionally complete food for target host species, 2) make food resources available at low densities for reduced time periods at unpredictable sites to avoid individual concentration, which can increase pathogen transmission, and 3) avoid feeding activities during epidemics, host migration, and birth pulses.

Characterizing the spreading abilities of host individuals and, in particular, identifying super-spreaders is of high interest for disease managers because control strategies targeting super-spreaders will greatly increase the efficiency of control efforts compared to population-level strategies (Lloyd-Smith et al., 2005). We found that migrating and dispersing Arctic foxes had more chance than nomadic and sedentary Arctic foxes to act as super-spreaders. The multi-annual cycles of lemming populations may shape large-scale movements of Arctic foxes (Angerbjorn et al., 1999; Norén et al., 2011). In particular, after a lemming peak, a large number of lemming foxes may move over long distances across sea ice and immigrate into coastal habitats (Norén et al., 2011). We expect that contact dynamics change when temporal fluctuations in prey resources are incorporated into the ABM. The cyclic nature of lemming populations is likely to affect the dynamics of rabies epizootics in a complex way. For example, Simon et al. (2019) found that strong demographic fluctuations in prey populations induced less regular and more intense rabies outbreaks, with rabies epizootics not following the pattern of Arctic fox density. However, there is little knowledge about seasonal variations in contact rates among Arctic foxes (Simon et al., 2020). In addition, the main ecological drivers of large-scale movements of Arctic foxes are still unclear and more research is needed to identify them (Lai et al., 2017). Ideally, denning sites for Arctic foxes in inland (lemming) habitats should be targeted for future rabies control interventions using ORV during the fall season, before foxes potentially disperse or migrate to resource hotspots across sea ice. The location of denning sites seems predictable as Arctic foxes select preferentially south-facing mounds or steep slopes, sandy substrate and streamside cutbanks to excavate their dens (Szor et al., 2008). However, to date, ORV planning is challenging due to the difficulty to find active dens with fox presence in High Arctic regions. Predicted probability maps of den site selection (e.g., Crupi et al., 2020; Davies et al., 2016) would be useful for identifying sites with a high probability of fox den presence and supporting ORV planning.

Our ABM describes density-dependent transmission of an infectious pathogen within a single host species. However, Arctic rabies can be maintained by a secondary reservoir species, the red fox (*Vulpes vulpes*), which has expanded its range into habitats occupied by the Arctic fox (Elmhagen et al., 2017; Simon et al., 2019). This range expansion can be attributed to an increase in food resources resulting from climate warming and increased human activities in the North (Elmhagen et al., 2017; Gallant et al., 2020; Hersteinsson and MacDonald, 1992). Red foxes and Arctic foxes compete for food and shelters, which can lead to interference competition through aggression and predation by the red fox (Elmhagen et al., 2002; Pamperin et al., 2006; Rodnikova et al., 2011), and thus increase the risk of rabies virus transmission between the two species. Our ABM could be extended by incorporating multiple species and real landscapes to achieve a better understanding of the consequences of environmental changes on spread and transmission dynamics of rabies in the Arctic. The application of the ABM to such a more complex system will be an important next step in this line of research.

Data accessibility

The Argos data are available in MoveBank (www.movebank.org) and stored in the MoveBank Data Repository (https://doi.org/10.5441/001/1.3gg33bd4) (**Berteaux, 2021**).

Funding

This work was funded by a Natural Sciences and Engineering Research Council of Canada (NSERC) Discovery grant to P.A.L. Field data collection was funded by many sources providing grants to D.B., including the Network of Centers of Excellence of Canada ArcticNet.

CRediT authorship contribution statement

Olivia Tardy: Conceptualization, Methodology, Software, Validation, Formal analysis, Investigation, Data curation, Writing – original draft, Writing – review & editing, Visualization, Supervision. **Christophe Lenglos:** Conceptualization, Writing – review & editing, Visualization. **Sandra Lai:** Conceptualization, Writing – review & editing. **Dominique Berteaux:** Conceptualization, Writing – review & editing, Funding acquisition. **Patrick A. Leighton:** Conceptualization, Writing – review & editing, Supervision, Funding acquisition.

Declaration of Competing Interest

The authors declare that they have no known competing financial interests or personal relationships that could have appeared to influence the work reported in this paper.

Data Availability

Data and code will be made available on request.

Acknowledgments

We are grateful for the computational resources provided by Calcul Québec (https://www.calculquebec.ca/) and Compute Canada (https://www.computecanada.ca/). All simulations were run on the Cedar supercomputer (Simon Fraser University), which is managed by Compute Canada. We would like to thank Daniel Stubbs for the excellent technical support.

Supplementary materials

Supplementary material associated with this article can be found, in the online version, at doi:10.1016/j.ecolmodel.2022.110207.

References

Aarts, G., Fieberg, J., Brasseur, S., Matthiopoulos, J., 2013. Quantifying the effect of habitat availability on species distributions. J. Anim. Ecol. 82, 1135–1145.
Altizer, S., Becker, D.J., Epstein, J.H., Forbes, K.M., Gillespie, T.R., Hall, R.J., Hawley, D. M., Hernandez, S.M., Martin, L.B., Plowright, R.K., Satterfield, D.A., Streicker, D.G., 2018. Food for contagion: synthesis and future directions for studying host-parasite responses to resource shifts in anthropogenic environments. Philos. Trans. R. Soc. B: Biol. Sci. 373, 20170102.
Altizer, S., Nunn, C.L., Thrall, P.H., Gittleman, J.L., Antonovics, J., Cunningham, A.A., Dobson, A.P., Ezenwa, V., Jones, K.E., Pedersen, A.B., Poss, M., Pulliam, J.R.C., 2003. Social organization and parasite risk in mammals: integrating theory and empirical studies. Annu. Rev. Ecol. Evol. Syst. 34, 517–547.
Angerbjörn, A., Hersteinsson, P., Tannerfeldt, M., 2004. Consequences of resource predictability in the Arctic fox: two life history strategies. In: Macdonald, D.W., Sillero-Zubiri, C. (Eds.), The Biology and Conservation of Wild Canids, eds. Oxford University Press, Oxford, England, pp. 163–172.
Angerbjorn, A., Tannerfeldt, M., Erlinge, S., 1999. Predator–prey relationships: arctic foxes and lemmings. J. Anim. Ecol. 68, 34–49.
Baer, G.M., 1991. The Natural History of Rabies, 2nd ed. CRC press, Boston, United States of America, p. 640.
Ballard, W.B., Follmann, E.H., Ritter, D.G., Robards, M.D., Cronin, M.A., 2001. Rabies and canine distemper in an arctic fox population in Alaska. J. Wildl. Dis. 37, 133–137.
Bastille-Rousseau, G., Potts, J.R., Yackulic, C.B., Frair, J.L., Ellington, E.H., Blake, S., 2016. Flexible characterization of animal movement pattern using net squared displacement and a latent state model. Mov. Ecol. 4, 15.
Bauduin, S., McIntire, E.J.B., Chubaty, A.M., 2019. NetLogoR: a package to build and run spatially explicit agent-based models in R. Ecography 42, 1841–1849.
Becker, D.J., Streicker, D.G., Altizer, S., 2015. Linking anthropogenic resources to wildlife–pathogen dynamics: a review and meta-analysis. Ecol. Lett. 18, 483–495.
Benhamou, S., 2014. Of scales and stationarity in animal movements. Ecol. Lett. 17, 261–272.
Berteaux, D., 2021. Data from: Study "Arctic Fox Bylot-Argos tracking". Movebank Data Repository. Available at. https://www.datarepository.movebank.org/handle/10255/move.1271.
Berteaux, D., Casajus, N., Angerbjörn, A., Fuglei, E., 2017. Foreword to supplement 1: research on a polar species–the Arctic fox. Polar Res 36, 1.
Bêty, J., Gauthier, G., Korpimäki, E., Giroux, J.-.F., 2002. Shared predators and indirect trophic interactions: lemming cycles and arctic-nesting geese. J. Anim. Ecol. 71, 88–98.
Bian, L., 2003. The representation of the environment in the context of individual-based modeling. Ecol. Model. 159, 279–296.
Blancou, J., Artois, M., Gilot-Fromont, E., Kaden, V., Rossi, S., Smith, G.C., Hutchings, M. R., Chambers, M.A., Houghton, S., Delahay, R.J., 2009. Options for the control of disease 1: targeting the infectious or parasitic agent. In: Delahay, R., Smith, G.C., Hutchings, M.R. (Eds.), Management of Disease in Wild Mammals, eds. Springer, Tokyo, Japan, pp. 97–120.
Bocedi, G., Zurell, D., Reineking, B., Travis, J.M.J., 2014. Mechanistic modelling of animal dispersal offers new insights into range expansion dynamics across fragmented landscapes. Ecography 37, 1240–1253.
Bonte, D., Van Dyck, H., Bullock, J.M., Coulon, A., Delgado, M., Gibbs, M., Lehouck, V., Matthysen, E., Mustin, K., Saastamoinen, M., Schtickzelle, N., Stevens, V.M., Vandewoestijne, S., Baguette, M., Barton, K., Benton, T.G., Chaput-Bardy, A., Clobert, J., Dytham, C., Hovestadt, T., Meier, C.M., Palmer, S.C.F., Turlure, C., Travis, J.M.J., 2012. Costs of dispersal. Biol. Rev. 87, 290–312.
Boulinier, T., Kada, S., Ponchon, A., Dupraz, M., Dietrich, M., Gamble, A., Bourret, V., Duriez, O., Bazire, R., Tornos, J., 2016. Migration, prospecting, dispersal? What host movement matters for infectious agent circulation? Integr. Comp. Biol. 56, 330–342.
Bracis, C., Gurarie, E., Van Moorter, B., Goodwin, R.A., 2015. Memory effects on movement behavior in animal foraging. PLoS ONE 10, e0136057.
Brunker, K., Lemey, P., Marston, D.A., Fooks, A.R., Lugelo, A., Ngeleja, C., Hampson, K., Biek, R., 2018. Landscape attributes governing local transmission of an endemic zoonosis: rabies virus in domestic dogs. Mol. Ecol. 27, 773–788.
Bunnefeld, N., Börger, L., Van Moorter, B., Rolandsen, C.M., Dettki, H., Solberg, E.J., Ericsson, G., 2011. A model-driven approach to quantify migration patterns: individual, regional and yearly differences. J. Anim. Ecol. 80, 466–476.
Civitello, D.J., Allman, B.E., Morozumi, C., Rohr, J.R., 2018. Assessing the direct and indirect effects of food provisioning and nutrient enrichment on wildlife infectious disease dynamics. Philos. Trans. R. Soc. B: Biol. Sci. 373, 20170101.
Crandell, R.A., 1991. Arctic fox rabies. In: Baer, G.M. (Ed.), The Natural History of Rabies, ed. CRC Press, Boca Raton, United States of America, pp. 291–306.
Crupi, A.P., Gregovich, D.P., White, K.S., 2020. Steep and deep: terrain and climate factors explain brown bear (*Ursus arctos*) alpine den site selection to guide heli-skiing management. PLoS ONE 15, e0238711.
Davies, A.B., Marneweck, D.G., Druce, D.J., Asner, G.P., 2016. Den site selection, pack composition, and reproductive success in endangered African wild dogs. Behav. Ecol. 27, 1869–1879.
Dougherty, E.R., Seidel, D.P., Carlson, C.J., Spiegel, O., Getz, W.M., 2018. Going through the motions: incorporating movement analyses into disease research. Ecol. Lett. 21, 588–604.
Dupont, G., Linden, D.W., Sutherland, C., 2021. Improved inferences about landscape connectivity from spatial capture–recapture by integration of a movement model. Ecology e03544.
Elith, J., Leathwick, J.R., Hastie, T., 2008. A working guide to boosted regression trees. J. Anim. Ecol. 77, 802–813.
Elmhagen, B., Berteaux, D., Burgess, R.M., Ehrich, D., Gallant, D., Henttonen, H., Ims, R. A., Killengreen, S.T., Niemimaa, J., Norén, K., Ollila, T., Rodnikova, A., Sokolov, A. A., Sokolova, N.A., Stickney, A.A., Angerbjörn, A., 2017. Homage to Hersteinsson and Macdonald: climate warming and resource subsidies cause red fox range expansion and Arctic fox decline. Polar Res 36, 3.
Elmhagen, B., Tannerfeldt, M., Angerbjörn, A., 2002. Food-niche overlap between arctic and red foxes. Can. J. Zool. 80, 1274–1285.
Elmore, S.A., Chipman, R.B., Slate, D., Huyvaert, K.P., VerCauteren, K.C., Gilbert, A.T., 2017. Management and modeling approaches for controlling raccoon rabies: the road to elimination. PLoS Negl. Trop. Dis. 11, e0005249.
Fofana, A.M., Hurford, A., 2017. Mechanistic movement models to understand epidemic spread. Philos. Trans. R. Soc. B: Biol. Sci. 372, 20160086.
Follmann, E., Ritter, D., Swor, R., Dunbar, M., Hueffer, K., 2011. Preliminary evaluation of raboral V-RG® oral rabies vaccine in Arctic foxes (*Vulpes lagopus*). J. Wildl. Dis. 47, 1032–1035.
Follmann, E.H., Ritter, D.G., Donald, W.H., 2004. Oral vaccination of captive arctic foxes with lyophilized SAG2 rabies vaccine. J. Wildl. Dis. 40, 328–334.
Fooks, A.R., Banyard, A.C., Horton, D.L., Johnson, N., McElhinney, L.M., Jackson, A.C., 2014. Current status of rabies and prospects for elimination. Lancet 384, 1389–1399.
Forester, J.D., Im, H.K., Rathouz, P.J., 2009. Accounting for animal movement in estimation of resource selection functions: sampling and data analysis. Ecology 90, 3554–3565.
Fritzsche McKay, A., Hoye, B.J., 2016. Are migratory animals superspreaders of infection? Integr. Comp. Biol. 56, 260–267.
Fryxell, J.M., Hazell, M., Börger, L., Dalziel, B.D., Haydon, D.T., Morales, J.M., McIntosh, T., Rosatte, R.C., 2008. Multiple movement modes by large herbivores at multiple spatiotemporal scales. Proc. Natl. Acad. Sci. U. S. A. 105, 19114–19119.
Fuglei, E., Tarroux, A., 2019. Arctic fox dispersal from Svalbard to Canada: one female's long run across sea ice. Polar Res 38, 3512.

Gallant, D., Lecomte, N., Berteaux, D., 2020. Disentangling the relative influences of global drivers of change in biodiversity: a study of the twentieth-century red fox expansion into the Canadian Arctic. J. Anim. Ecol. 89, 565–576.
Grimm, V., Berger, U., Bastiansen, F., Eliassen, S., Ginot, V., Giske, J., Goss-Custard, J., Grand, T., Heinz, S.K., Huse, G., Huth, A., Jepsen, J.U., Jørgensen, C., Mooij, W.M., Müller, B., Pe'er, G., Piou, C., Railsback, S.F., Robbins, A.M., Robbins, M.M., Rossmanith, E., Rüger, N., Strand, E., Souissi, S., Stillman, R.A., Vabø, R., Visser, U., DeAngelis, D.L., 2006. A standard protocol for describing individual-based and agent-based models. Ecol. Model. 198, 115–126.
Grimm, V., Berger, U., DeAngelis, D.L., Polhill, J.G., Giske, J., Railsback, S.F., 2010. The ODD protocol: a review and first update. Ecol. Model. 221, 2760–2768.
Grimm, V., Railsback, S.F., Vincenot, C.E., Berger, U., Gallagher, C., DeAngelis, D.L., Edmonds, B., Ge, J., Giske, J., Groeneveld, J., Johnston, A.S.A., Milles, A., Nabe-Nielsen, J., Polhill, J.G., Radchuk, V., Rohwäder, M.-S., Stillman, R.A., Thiele, J.C., Ayllón, D., 2020. The ODD protocol for describing agent-based and other simulation models: a second update to improve clarity, replication, and structural realism. J. Artif. Soc. Soc. Simul. 23, 7.
Hall, R.J., Altizer, S., Bartel, R.A., 2014. Greater migratory propensity in hosts lowers pathogen transmission and impacts. J. Anim. Ecol. 83, 1068–1077.
Hampson, K., Coudeville, L., Lembo, T., Sambo, M., Kieffer, A., Attlan, M., Barrat, J., Blanton, J.D., Briggs, D.J., Cleaveland, S., Costa, P., Freuling, C.M., Hiby, E., Knopf, L., Leanes, F., Meslin, F.-X., Metlin, A., Miranda, M.E., Müller, T., Nel, L.H., Recuenco, S., Rupprecht, C.E., Schumacher, C., Taylor, L., Vigilato, M.A.N., Zinsstag, J., Dushoff, J., 2015. Estimating the global burden of endemic canine rabies. PLoS Negl. Trop. Dis. 9, e0003709.
Hersteinsson, P., MacDonald, D.W., 1992. Interspecific competition and the geographical distribution of red and Arctic foxes *Vulpes vulpes* and *Alopex lagopus*. Oikos 64, 505–515.
Hersteinsson, P., Macdonald, D.W., 1996. Diet of arctic foxes (*Alopex lagopus*) in Iceland. J. Zool. 240, 457–474.
Hijmans, R.J., Phillips, S., Leathwick, J., Elith, J., 2020. dismo: species distribution modeling. R package version 1.3-3. Available at https://CRAN.R-project.org/package=dismo.
Johnson, C.J., Seip, D.R., Boyce, M.S., 2004. A quantitative approach to conservation planning: using resource selection functions to map the distribution of mountain caribou at multiple spatial scales. J. Appl. Ecol. 41, 238–251.
Johnson, D.S., London, J.M., Lea, M.-A., Durban, J.W., 2008. Continuous-time correlated random walk model for animal telemetry data. Ecology 89, 1208–1215.
Johnson, P.T.J., Hoverman, J.T., 2014. Heterogeneous hosts: how variation in host size, behaviour and immunity affects parasite aggregation. J. Anim. Ecol. 83, 1103–1112.
Joo, R., Boone, M.E., Clay, T.A., Patrick, S.C., Clusella-Trullas, S., Basille, M., 2020. Navigating through the r packages for movement. J. Anim. Ecol. 89, 248–267.
Jouffray, J.-B., Wedding, L.M., Norström, A.V., Donovan, M.K., Williams, G.J., Crowder, L.B., Erickson, A.L., Friedlander, A.M., Graham, N.A.J., Gove, J.M., Kappel, C.V., Kittinger, J.N., Lecky, J., Oleson, K.L.L., Selkoe, K.A., White, C., Williams, I.D., Nyström, M., 2019. Parsing human and biophysical drivers of coral reef regimes. Proc. R. Soc. B 286, 20182544.
Konovalov, G.V., Kantorovich, R.A., Buzinov, I.A., Riutova, V.P., 1965. Experimental investigations into rage and rabies in polar foxes, natural hosts of the infection. II. An experimental morphological study of rabies in polar foxes. Acta Virol 9, 235–239.
Krylova, O., Earn, D.J.D., 2013. Effects of the infectious period distribution on predicted transitions in childhood disease dynamics. J. Royal Soc. Interface 10, 20130098.
Kun, Á., Scheuring, I., 2006. The evolution of density-dependent dispersal in a noisy spatial population model. Oikos 115, 308–320.
Lai, S., Bêty, J., Berteaux, D., 2015. Spatio–temporal hotspots of satellite–tracked arctic foxes reveal a large detection range in a mammalian predator. Mov. Ecol. 3, 1–10.
Lai, S., Bêty, J., Berteaux, D., 2017. Movement tactics of a mobile predator in a meta-ecosystem with fluctuating resources: the arctic fox in the High Arctic. Oikos 126, 937–947.
Langrock, R., King, R., Matthiopoulos, J., Thomas, L., Fortin, D., Morales, J.M., 2012. Flexible and practical modeling of animal telemetry data: hidden Markov models and extensions. 93, 2336–2342.
Lloyd-Smith, J.O., Schreiber, S.J., Kopp, P.E., Getz, W.M., 2005. Superspreading and the effect of individual variation on disease emergence. Nature 438, 355–359.
McClintock, B.T., 2021. Worth the effort? A practical examination of random effects in hidden Markov models for animal telemetry data. Methods Ecol. Evol. 12, 1475–1497.
McClintock, B.T., Michelot, T., 2018. momentuHMM: R package for generalized hidden Markov models of animal movement. Methods Ecol. Evol. 9, 1518–1530.
McClure, K.M., Bastille-Rousseau, G., Davis, A.J., Stengel, C.A., Nelson, K.M., Chipman, R.B., Wittemyer, G., Abdo, Z., Gilbert, A.T., Pepin, K.M., 2022. Accounting for animal movement improves vaccination strategies against wildlife disease in heterogeneous landscapes. Ecol. Appl. 32, e2568.
McClure, K.M., Gilbert, A.T., Chipman, R.B., Rees, E.E., Pepin, K.M., 2020. Variation in host home range size decreases rabies vaccination effectiveness by increasing the spatial spread of rabies virus. J. Anim. Ecol. 89, 1375–1386.
McKay, M.D., Beckman, R.J., Conover, W.J., 1979. Comparison of three methods for selecting values of input variables in the analysis of output from a computer code. Technometrics 21, 239–245.
Mediouni, S., Brisson, M., Ravel, A., 2020. Epidemiology of human exposure to rabies in Nunavik: incidence, the role of dog bites and their context, and victim profiles. BMC Public Health 20, 584.
Michelot, T., Langrock, R., Bestley, S., Jonsen, I.D., Photopoulou, T., Patterson, T.A., 2017. Estimation and simulation of foraging trips in land-based marine predators. Ecology 98, 1932–1944.
Michelot, T., Langrock, R., Patterson, T.A., 2016. moveHMM: an R package for the statistical modelling of animal movement data using hidden Markov models. Methods Ecol. Evol. 7, 1308–1315.
Moran, E.J., Lecomte, N., Leighton, P., Hurford, A., 2021. Understanding rabies persistence in low-density fox populations. Ecoscience 28, 301–312.
Moran, E.J., Martignoni, M.M., Lecomte, N., Leighton, P., Hurford, A., 2022. When Host Populations Move north, But Disease Moves South: Counter-Intuitive Impacts of Climate Warming on Disease Spread. bioRxiv, 2022.2001.2026.477883.
Mørk, T., Prestrud, P., 2004. Arctic rabies – a review. Acta Vet. Scand. 45, 1.
Murray, M.H., Becker, D.J., Hall, R.J., Hernandez, S.M., 2016. Wildlife health and supplemental feeding: a review and management recommendations. Biol. Conserv. 204, 163–174.
Newton, E.J., Pond, B.A., Tinline, R.R., Middel, K., Bélanger, D., Rees, E.E., 2019. Differential impacts of vaccination on wildlife disease spread during epizootic and enzootic phases. J. Appl. Ecol. 56, 526–536.
Norén, K., Carmichael, L., Fuglei, E., Eide, N.E., Hersteinsson, P., Angerbjörn, A., 2011. Pulses of movement across the sea ice: population connectivity and temporal genetic structure in the arctic fox. Oecologia 166, 973–984.
Pamperin, N.J., Follmann, E.H., Petersen, B., 2006. Interspecific killing of an Arctic fox by a red fox at Prudhoe Bay, Alaska. Arctic 59, 361–364.
Pinsky, M.L., Byler, D., 2015. Fishing, fast growth and climate variability increase the risk of collapse. Proc. R. Soc. B 282, 20151053.
Pohle, J., Langrock, R., van Beest, F.M., Schmidt, N.M., 2017. Selecting the number of states in hidden Markov models: pragmatic solutions illustrated using animal movement. J. Agric. Biol. Environ. Stat. 22, 270–293.
Prestrud, P., 1992. Food habits and observations of the hunting behaviour of arctic foxes, *Alopex lagopus*. Svalbard. Can. Field-Nat. 106, 225–236.
Prestrud, P., Krogsrud, J., Gjertz, I., 1992. The occurrence of rabies in the Svalbard Islands of Norway. J. Wildl. Dis. 28, 57–63.
Pruvot, M., Lejeune, M., Kutz, S., Hutchins, W., Musiani, M., Massolo, A., Orsel, K., 2016. Better alone or in ill company? The effect of migration and inter-species comingling on Fascioloides magna infection in elk. PLoS ONE 11, e0159319.
R Development Core Team, 2019. R: A Language and Environment for Statistical Computing. R Foundation for Statistical Computing, Vienna, Austria. Available at. http://www.R-project.org.
Rausch, R.L., 1972. Observations on some natural-focal zoonoses in Alaska. Arch. Environ. Health: Int. J. 25, 246–252.
Rayl, N.D., Merkle, J.A., Proffitt, K.M., Almberg, E.S., Jones, J.D., Gude, J.A., Cross, P.C., 2021. Elk migration influences the risk of disease spillover in the Greater Yellowstone ecosystem. J. Anim. Ecol. 90, 1264–1275.
Risely, A., Klaassen, M., Hoye, B.J., 2018. Migratory animals feel the cost of getting sick: a meta-analysis across species. J. Anim. Ecol. 87, 301–314.
Rodnikova, A., Ims, R.A., Sokolov, A., Skogstad, G., Sokolov, V., Shtro, V., Fuglei, E., 2011. Red fox takeover of arctic fox breeding den: an observation from Yamal Peninsula, Russia. Polar Biol. 34, 1609.
Sararat, C., Changruenngam, S., Chumkaeo, A., Wiratsudakul, A., Pan-ngum, W., Modchang, C., 2022. The effects of geographical distributions of buildings and roads on the spatiotemporal spread of canine rabies: an individual-based modeling study. PLoS Negl. Trop. Dis. 16, e0010397.
Sardá-Espinosa, A., 2019. Time-series clustering in R using the dtwclust package. R J. 11, 22–43.
Satterfield, D.A., Marra, P.P., Sillett, T.S., Altizer, S., 2018. Responses of migratory species and their pathogens to supplemental feeding. Philos. Trans. R. Soc. B: Biol. Sci. 373, 20170094.
Shaw, A.K., Sherman, J., Barker, F.K., Zuk, M., 2018. Metrics matter: the effect of parasite richness, intensity and prevalence on the evolution of host migration. Proc. R. Soc. B 285, 20182147.
Simon, A., Bélanger, D., Berteaux, D., Hueffer, K., Rees, E., Leighton, P.A., 2020. Ecology of rabies in the Arctic fox (*Vulpes lagopus*). In: Gregory, D.J., Tinline, R.R. (Eds.), Taking the Bite Out of Rabies: The Evolution of Rabies Management in Canada, eds. University of Toronto Press, Toronto, Canada, pp. 453–465.
Simon, A., Tardy, O., Hurford, A., Lecomte, N., Bélanger, D., Leighton, P., 2019. Dynamics and persistence of rabies in the Arctic. Polar Res 38, 3366.
Smith, D.L., Lucey, B., Waller, L.A., Childs, J.E., Real, L.A., 2002. Predicting the spatial dynamics of rabies epidemics on heterogeneous landscapes. Proc. Natl. Acad. Sci. U. S. A. 99, 3668–3672.
Smith, M.J., Telfer, S., Kallio, E.R., Burthe, S., Cook, A.R., Lambin, X., Begon, M., 2009. Host-pathogen time series data in wildlife support a transmission function between density and frequency-dependence. Proc. Natl. Acad. Sci. U. S. A. 106, 7905–7909.
Sterner, R.T., Smith, G.C., 2006. Modelling wildlife rabies: transmission, economics, and conservation. Biol. Conserv. 131, 163–179.
Szor, G., Berteaux, D., Gauthier, G., 2008. Finding the right home: distribution of food resources and terrain characteristics influence selection of denning sites and reproductive dens in arctic foxes. Polar Biol 31, 351–362.
Tannerfeldt, M., Angerbjörn, A., 1998. Fluctuating resources and the evolution of litter size in the arctic fox. Oikos 83, 545–559.
Tardy, O., Bouchard, C., Chamberland, E., Fortin, A., Lamirande, P., Ogden, N.H., Leighton, P.A., 2021. Mechanistic movement models reveal ecological drivers of tick-borne pathogen spread. J. Royal Soc. Interface 18, 20210134.
Tardy, O., Massé, A., Pelletier, F., Fortin, D., 2018. Interplay between contact risk, conspecific density, and landscape connectivity: an individual-based modeling framework. Ecol. Model. 373, 25–38.
Tardy, O., Vincenot, C.E., Bouchard, C., Ogden, N.H., Leighton, P.A., 2022. Context-dependent host dispersal and habitat fragmentation determine heterogeneity in infected tick burdens: an agent-based modelling study. R. Soc. Open Sci. 9, 220245.

Tarroux, A., Berteaux, D., Bêty, J., 2010. Northern nomads: ability for extensive movements in adult arctic foxes. Polar Biol 33, 1021–1026.
Teitelbaum, C.S., Huang, S., Hall, R.J., Altizer, S., 2018. Migratory behaviour predicts greater parasite diversity in ungulates. Proc. R. Soc. B 285, 20180089.
Turchin, P., 1998. Quantitative Analysis of Movement: Measuring and Modeling Population Redistribution in Animals and Plants. Sinauer Associates, Sunderland, United States of America, p. 396 pp.
VanderWaal, K.L., Ezenwa, V.O., 2016. Heterogeneity in pathogen transmission: mechanisms and methodology. Funct. Ecol. 30, 1606–1622.
Warrell, M.J., Warrell, D.A., 2004. Rabies and other lyssavirus diseases. Lancet 363, 959–969.
Wilson, K., Bjørnstad, O.N., Dobson, A.P., Merler, S., Poglayen, G., Randolph, S.E., Read, A.F., Skorping, A., 2002. Heterogeneities in macroparasite infections: patterns and processes. In: Hudson, P.J., Rizzoli, A., Grenfell, B.T., Heesterbeek, H., Dobson, A.P. (Eds.), The Ecology of Wildlife Diseases, eds. Oxford University Press, New York, United States of America, pp. 6–44.
Woolhouse, M.E.J., Dye, C., Etard, J.-F., Smith, T., Charlwood, J.D., Garnett, G.P., Hagan, P., Hii, J.L.K., Ndhlovu, P.D., Quinnell, R.J., Watts, C.H., Chandiwana, S.K., Anderson, R.M., 1997. Heterogeneities in the transmission of infectious agents: implications for the design of control programs. Proc. Natl. Acad. Sci. U. S. A. 94, 338–342.
Zucchini, W., MacDonald, I.L., Langrock, R., 2017. Hidden Markov Models For Time Series: An Introduction Using R Second ed. CRC press, Boca Raton, United States of America, p. 288 pp.